UNCLASSIFIED

SECURITY CLASSIFICATION OF THIS PAGE

REPORT DOCUMENTATION PAGE

Form Approved OMB No. 0704-0188

1a. REPORT SECURITY CLASSIFICATION: UNCLASSIFIED	1b. RESTRICTIVE MARKINGS
2a. SECURITY CLASSIFICATION AUTHORITY	3. DISTRIBUTION/AVAILABILITY OF REPORT: Approved for public release; distribution unlimited
2b. DECLASSIFICATION/DOWNGRADING SCHEDULE	
4. PERFORMING ORGANIZATION REPORT NUMBER(S): HDL-TR-2139	5. MONITORING ORGANIZATION REPORT NUMBER(S)
6a. NAME OF PERFORMING ORGANIZATION: Harry Diamond Laboratories; 6b. OFFICE SYMBOL (If applicable): SLCHD-ST-SA	7a. NAME OF MONITORING ORGANIZATION
6c. ADDRESS (City, State, and ZIP Code): 2800 Powder Mill Road, Adelphi, MD 20783-1197	7b. ADDRESS (City, State, and ZIP Code)
8a. NAME OF FUNDING/SPONSORING ORGANIZATION: U.S. Army Laboratory Command; 8b. OFFICE SYMBOL (If applicable): AMSLC	9. PROCUREMENT INSTRUMENT IDENTIFICATION NUMBER
8c. ADDRESS (City, State, and ZIP Code): 2800 Powder Mill Road, Adelphi, MD 20783-1145	10. SOURCE OF FUNDING NUMBERS: PROGRAM ELEMENT NO. P611102.H44; PROJECT NO. AH44; TASK NO.; WORK UNIT ACCESSION NO.

11. TITLE (Include Security Classification): Rapid Backscatter Simulation Techniques for Detailed B-Spline Target Models

12. PERSONAL AUTHOR(S): Karl D. Reinig

13a. TYPE OF REPORT	13b. TIME COVERED	14. DATE OF REPORT (Year, Month, Day)	15. PAGE COUNT
Final	FROM Oct 85 TO July 87	December 1988	57

16. SUPPLEMENTARY NOTATION: HDL project: AE1814, AMS Code: 611102.H4400

17. COSATI CODES		
FIELD	GROUP	SUB-GROUP
12	01	
17	09	

18. SUBJECT TERMS (Continue on reverse if necessary and identify by block number): B-splines, radar backscatter, target models, backscatter simulation target encounter, geometric optics

19. ABSTRACT (Continue on reverse if necessary and identify by block number)

The report describes a method for rapidly evaluating the simulated radar backscatter signatures of B-spline target models moving relative to a source/receiver. A geometric optics approach is used to estimate the radar return from a complex target surface described by a bicubic B-spline mesh. The method exploits the second-order continuity of bicubic B-spline surfaces to reduce the problem of finding all the specular points associated with each new trajectory position to that of tracking the motion of existing points. In particular, it is shown that the locations of the annihilations and creations of specular paths may be predicted for an entire trajectory, eliminating the need to search the whole surface for specular points as the target moves in relation to the source/receiver. The method is shown to work for the multiple-bounce case as well. The report contains several recommendations for further exploitation of the properties of B-spline surfaces for the tracking of specular points.

20. DISTRIBUTION/AVAILABILITY OF ABSTRACT	21. ABSTRACT SECURITY CLASSIFICATION
☒ UNCLASSIFIED/UNLIMITED ☐ SAME AS RPT. ☐ DTIC USERS	UNCLASSIFIED
22a. NAME OF RESPONSIBLE INDIVIDUAL: Karl Reinig	22b. TELEPHONE (Include Area Code): (202)394-3140; 22c. OFFICE SYMBOL: SLCHD-ST-SA

DD Form 1473, JUN 86 — Previous editions are obsolete. — SECURITY CLASSIFICATION OF THIS PAGE: UNCLASSIFIED

Contents

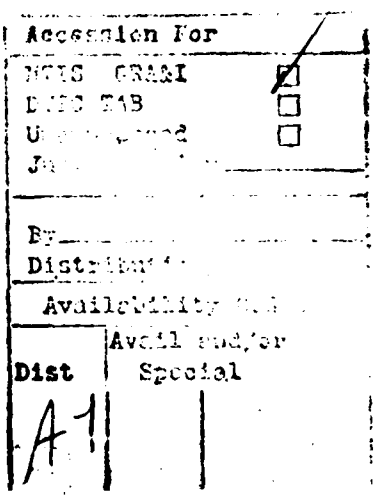

Appendices

Figures

1. Introduction

1.1 Problem Scenario

The expanding technology base exploiting millimeter and near-millimeter electromagnetic waves has greatly enhanced the ability of remote sensors to detect and identify complex targets of interest. The enhancement is especially significant when the target is obscured by fog, clouds, or smoke which can render infrared and optically based sensors useless. As a result, a large number of sensors operating at millimeter and near-millimeter wavelengths have been produced for such applications as identification of targets, terminal guidance, and fuzing. Accordingly, the need for efficient and informative simulation techniques for these high-frequency sensors has also risen. Consider the scenario depicted in figure 1.

A source/receiver (S/R) moving along some trajectory illuminates a target of interest. It is desired to estimate the return from the target as the S/R moves along the trajectory. Notice that whether figure 1 describes a target detection/identification problem or the terminal phase of a guided munition is mostly determined by the trajectory being considered. A backscatter simulation technique which places few or no restrictions on the paths of the trajectories to be simulated

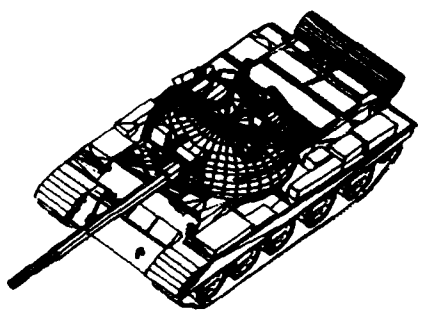

Figure 1: Target encounter scenario.

could therefore find use in all phases of seeker munitions studies. In addition, of course, the relative motion between the S/R and the target could be due strictly to the motion of the target. Thus the scenario could also include the return from passing targets. It will be assumed that the return should be calculated about a thousand times per meter of trajectory. The reason for mentioning this detail here is to introduce early the impact of the trajectory on any practical modeling method. In particular, this study attempts to include the trajectory into the structure of the problem, as opposed to simply considering the trajectory as a sequence of points at which to evaluate the return.

This report begins with a brief review of a modeling method developed at the Harry Diamond Laboratories for the computer simulation of fuze/air-target encounters. The simulation technique uses a composite of simple analytic structures (cones, spheres, flat plates, etc) to model the surface of a target of interest. A geometric optics assumption is then used to estimate the expected amplitude and phase of the return as the S/R moves along the trajectory of interest. The current study makes use of bicubic B-spline patches to describe arbitrary complex targets in greater detail. Using the geometric optics approach for estimating the target return, the backscatter problem becomes one of finding all the specular points of such an arbitrary surface with respect to the S/R location.

The main portion of this report describes a method for exploiting the continuity of the resulting surface model to reduce the problem of finding all the specular points associated with each new trajectory position to that of tracking the motion of existing points. In particular, it is shown that the locations of the annihilations and creations of specular paths may be predicted for an entire trajectory, eliminating the need to search the whole surface for specular points as the target moves in relation to the S/R. It is further shown that the same technique can be extended to include so-called multiple-bounce return, in which it is assumed that the signal is reflected about the surface two or more times before returning to the receiver. The general flow of simple algorithms for the implementation of the new strategy is described and the results of example runs displayed. The examples point out potential robustness problems with the simplistic algorithms, problems which are not inherent in the modeling method itself. The final section of the report outlines potential solutions to these problems as well as extensions to the model. The potential solutions and exten-

sions are presented as part of the suggested areas of further research and include

- the potential for further exploitation of the properties of bicubic B-spline surfaces to increase the robustness of the specular tracking algorithms,
- extensions to include surface discontinuities,
- extensions to include multiple bodies and shadowing, and
- experimental validation and comparison with other methods.

1.2 A Useful Backscatter Modeling Technique

Methods for developing radar backscatter models of air targets suitable for computer simulation of radar-fuze/air-target encounters are described by Dammann [1]. The models are developed in three steps:

> *First, the target is approximated by an ensemble of simple geometric shapes such as ogives, cylinders, flat plates, and ellipsoids. Second, the specular point (the point where the surface is perpendicular to the incident rays) is located on each shape. All the return is assumed to come from these specular points, and the strength of the return from each point is assumed to depend on the local curvatures of the surface at that point. Third, the returns from all specular points are summed vectorially to yield the total target return.* [1]

This modeling method has proved to be very useful both for predicting the backscatter characteristics of interest in fuze design and for the simulation of fuze processors. In particular, because the model provides actual Doppler voltage waveforms, the computer-generated waveforms can be fed directly into actual fuze processors to predict their response.

The target modeling technique described above has been particularly successful in the air-target encounter scenario partially because of the relative simplicity of the shapes of most aircraft. In many cases, between 10 and 20 primitive analytic shapes are all that are necessary to capture the essential shape of a particular aircraft. As the targets of interest become more complex or the desire to match their surface more accurately increases, the use of simple analytical shapes to describe the target surface often becomes impractical. Tensor-product

piecewise polynomial surfaces are a simple means of describing complex surfaces, and as such, present a practical way to extend the geometric optics approach to include targets of increased complexity.

1.3 Surface Modeling with B-splines

In this paper it is assumed that a three-dimensional vector function $\mathbf{R}(u,v)$ exists which describes the target surface of interest; that is, given a particular choice of u and v, $\mathbf{R}(u,v)$ represents the x-, y-, and z-coordinates of a point on the target surface. It is further assumed that over the entire domain of $\mathbf{R}$ (call this $U \times V$) the partial derivative vectors

$$\frac{\partial^{i+j}\mathbf{R}(u,v)}{\partial u^i \partial v^j} \tag{1}$$

exist and are continuous for $i + j \leq 2$. B-splines can be used to convert a patchwork of data points into just such a function. For the major results of this paper it is the second-order continuity of the surface which is exploited to reduce the backscatter simulation time, and an understanding of B-splines is really not necessary. However, the following brief discussion may be helpful. (The reader interested in the details of B-splines in general is encouraged to study de Boor's book *A Practical Guide to Splines* [2] or, for a quicker look, see Gordon and Riesenfeld [3], Cox [4], or Amos [5].)

The mathematical term "spline" originates from the mechanical spline used by draftsmen to trace out smooth curves. When thin strips of wood or metal are pinned at strategic locations on the drafting board, the material takes on a shape to minimize its internal stress and gives a generally pleasing interpolant to the data. If the draftsman is not pleased with the resulting trace, the number of pinning points and their locations may be altered until the desired shape is formed. Piecewise polynomial functions are the mathematical material of choice for fitting smooth curves through or near a given set of data. The term "piecewise" refers to breaking up the entire curve into sections of low-order polynomials (most often cubic). The sections are joined at "knots" so that appropriate continuity is maintained. The term "B-spline" refers to a special set of piecewise polynomial functions which form a basis for all piecewise polynomials having a given knot set and continuity constraints at the knots. As an example, the cubic B-spline basis functions with uniformly spaced knots having zeroth, first, and second derivative continuity at each of the knots may be written as

$$
\begin{aligned}
B_1(z) &= (1-z)^3/6, \\
B_2(z) &= (3z^3 - 6z^2 + 4)/6, \\
B_3(z) &= (-3z^3 + 3z^2 + 3z + 1)/6, \\
B_4(z) &= z^3/6.
\end{aligned}
$$

Note that a linear combination of the functions above can be used to construct any desired cubic polynomial. Now suppose that we have a rectangular mesh of points which we would like to use to describe a surface. The mesh can be used to form a tensor product surface using the same basis functions. Consider the behavior of the following function:

$$\mathbf{R}_{k,l}(u,v) = \sum_{i=1}^{4}\sum_{j=1}^{4} B_i(u)(\mathbf{\Lambda}_{i+k,j+l})B_j(v),$$

where $\mathbf{\Lambda}_{i+k,j+l}$ are three-dimensional vectors of finite length and u and v are real numbers ranging from 0 to 1. $\mathbf{R}_{k,l}(u,v)$ is simply one way of writing a bicubic B-spline surface defined over a uniform rectangular knot set for the k,lth patch of the quilt of data points. Clearly, for any fixed values of k and l, and for all u and $v \in (0,1)$, the various partial derivatives of equation (1) are continous functions of u and v for all positive integers i and j. It is also easy to verify that all the zeroth, first, and second partial derivatives with respect to u and v are continuous across neighboring values of k and l. For example,

$$
\begin{aligned}
\frac{\partial^2 R_{k,l}(u,v)}{\partial u \partial v} &= \sum_{i=1}^{4}\sum_{j=1}^{4} \frac{\partial B_i(u)}{\partial u}(\mathbf{\Lambda}_{i+k,j+l})\frac{\partial B_j(v)}{\partial v} \\
&= 1/4\Big\{-(1-u)^2[-(1-v)^2\mathbf{\Lambda}_{k+1,l+1} + (3v^2-4v)\mathbf{\Lambda}_{k+1,l+2} \\
&\quad +(-3v^2+2v+1)\mathbf{\Lambda}_{k+1,l+3} + v^2\mathbf{\Lambda}_{k+1,l+4}] \\
&\quad +(3u^2-4u)[-(1-v)^2\mathbf{\Lambda}_{k+2,l+1} + (3v^2-4v)\mathbf{\Lambda}_{k+2,l+2} \\
&\quad +(-3v^2+2v+1)\mathbf{\Lambda}_{k+2,l+3} + v^2\mathbf{\Lambda}_{k+2,l+4}] \\
&\quad +(-3u^2+2u+1)[-(1-v)^2\mathbf{\Lambda}_{k+3,l+1} + (3v^2-4v)\mathbf{\Lambda}_{k+3,l+2} \\
&\quad +(-3v^2+2v+1)\mathbf{\Lambda}_{k+3,l+3} + v^2\mathbf{\Lambda}_{k+3,l+4}] \\
&\quad +(u^2)[-(1-v)^2\mathbf{\Lambda}_{k+4,l+1} + (3v^2-4v)\mathbf{\Lambda}_{k+4,l+2} \\
&\quad +(-3v^2+2v+1)\mathbf{\Lambda}_{k+4,l+3} + v^2\mathbf{\Lambda}_{k+4,l+4}]\Big\},
\end{aligned}
$$

from which it is an easy check that

$$\begin{aligned}\frac{\partial^2 R_{k,l}(u,0)}{\partial u \partial v} &= 1/4\Big\{-(1-u)^2[\Lambda_{k+1,l+1}+\Lambda_{k+1,l+3}] \\ &\quad +(3u^2-4u)[\Lambda_{k+2,l+1}+\Lambda_{k+2,l+3}] \\ &\quad +(-3u^2+2u+1)[\Lambda_{k+3,l+1}+\Lambda_{k+3,l+3}] \\ &\quad +(u^2)[\Lambda_{k+4,l+1}+\Lambda_{k+4,l+3}]\Big\} \\ &= \frac{\partial^2 R_{k,l-1}(u,1)}{\partial u \partial v}.\end{aligned}$$

While many surface modeling methods offer smooth surfaces, the B-spline surface in general has three major properties which make it particularly well suited for surface modeling. The first is that the surface passes near (in a sense that will not be elaborated here) the points $\Lambda_{i,j}$. This allows the modeler to choose a mesh of points which generally describes the desired surface (much like a planar facet model) and then observe the resulting surface. As might be expected, the more points that are used to define the surface, the closer the surface will pass to the points. The second major property is the local influence of the points $\Lambda_{i,j}$; that is, a change in the position of the point $\Lambda_{i,j}$ only changes the surface near the point. The local nature of the spline allows the modeler to move points around to improve the surface in a particular area without modifying the rest of the model. The third major property, closely related to the first, is the variation-diminishing property of B-splines. Loosely speaking, the variation-diminishing property guarantees that any plane will cut through a three-dimensional B-spline curve no more times than it does a linear interpolant to the original data points.

It is the second-order continuity of the surface which is exploited for the main results of this paper. Since many other methods exist for representing smooth surfaces, the main results are more general than just for B-spline surfaces. However, mostly because of the previously stated B-spline properties, the surfaces exemplified in this report are all based on B-splines. In addition, a large portion of the suggested further research is aimed towards exploiting those properties specific to B-spline surfaces.

2. Geometric Optics Approach Using B-splines

2.1 Single-Bounce Return

The geometry of the specular return problem from a single patch of an arbitrary B-spline surface is shown in figure 2. $\mathbf{R}_t(\Delta)$ is the current position of the projectile along a linear trajectory, $\mathbf{R}_s(u,v)$ describes the target surface as a function of the two parameters u and v, and $\mathbf{G}(u,v,\Delta)$ is the difference between the two vectors $\mathbf{R}_t(\Delta)$ and $\mathbf{R}_s(u,v)$. It is assumed throughout the analysis that the projectile has an unobstructed view of the surface being considered (the problem of shadowing is ignored and addressed only in the section on suggested further research). A necessary and sufficient condition for a point on the surface to be a specular point relative to the position $\mathbf{R}_t(\Delta)$ is that the l_2 norm of $\mathbf{G}(u,v,\Delta)$ be either a local maximum or minimum with respect to the two target surface parameters u and v. Finding all the specular points of a given surface (for a given trajectory position) is therefore the same as finding all u and v that satisfy the two nonlinear equations

$$F_1(u,v,\Delta) = \frac{\partial \|\mathbf{G}(u,v,\Delta)\|^2}{\partial u} = 0 \tag{2}$$

and

$$F_2(u,v,\Delta) = \frac{\partial \|\mathbf{G}(u,v,\Delta)\|^2}{\partial v} = 0. \tag{3}$$

If $\mathbf{R}(u,v)$ is given by a tensor product of cubic B-splines on a uniform grid, both $F_1(u,v,\Delta)$ and $F_2(u,v,\Delta)$ may be written explicitly

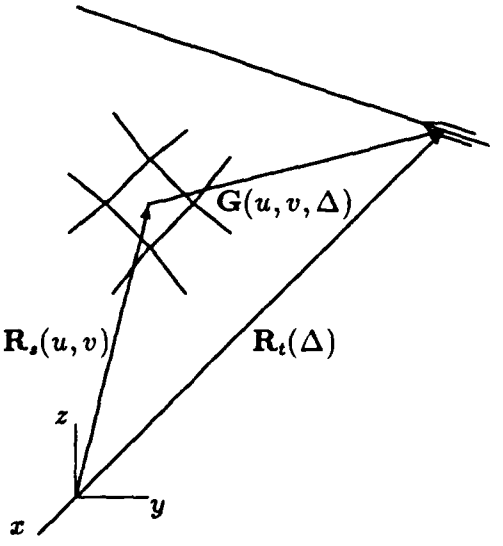

Figure 2: Specular return geometry.

in terms of u and v. However, the u and v which solve equations (2) and (3) (call them u^* and v^*) cannot be found explicitly, since $F_1(u,v)$ is a bivariate polynomial of degree five in u and six in v, while $F_2(u,v)$ is a bivariate polynomial of degree six in u and five in v. In general then, solving equations (2) and (3) for u^* and v^* requires a numerical technique. Simple application of Newton's method for nonlinear equations will find solutions to (2) and (3) provided the search is begun "close enough" to (u^*,v^*). The question of how close is close enough is a complex one which ultimately depends on the variation of the surface being considered. An explanation of Newton's method and algorithms which incorporate the method may be found in most optimization texts including Luenberger [6]. The essential step is to solve the following linear system of equations:

$$\mathbf{J}(u,v)\mathbf{S} = \mathbf{F}(u,v), \tag{4}$$

where $\mathbf{F}(u,v)$ is the 2×1 vector $[F_1(u,v), F_2(u,v)]^T$, $\mathbf{J}(u,v)$ is the 2×2 Jacobian of $\mathbf{F}(u,v)$ with respect to u and v, and $\mathbf{S}$ is the 2×1 vector for the new step in u and v. A derivation of the Newton step for the location of a specular point on a B-spline surface may be found in appendix A. It is easy to see that for the bicubic B-spline surface being considered, the elements of $\mathbf{J}(u,v)$ are continuous functions of u and v; that is, all second-order derivatives of $\mathbf{G}(u,v)$ exist and are continuous functions of u and v.

Using Newton's method alone, it would be possible to thoroughly search each B-spline patch for specular points, keeping track of their positions and local principal radii of curvatures for use in the geometric optics estimation of the return from the composite model. The procedure would have to be repeated for each new position along the trajectory. To get a feel for the time which may be required for a single simulation, suppose a target were being modeled by B-splines over an 80 by 50 knot grid (4000 patches, give or take a few end conditions) and that it were possible to thoroughly search 100 B-spline patches per second. The specular return from the target could be calculated in approximately 40 s for one point along the trajectory of interest. Now suppose further that we are interested in a 10-m trajectory to be sampled at 1-mm increments (not an unlikely requirement when working with millimeter waves). The simulation of the signature for the single trajectory would take approximately 400,000 s, or a little over four and one half days. Admittedly, other techniques could probably be used to cut down on the time required to search the composite

model for specular points. (Methods based on recursive subdivision of the target surface using, for example, the Oslo algorithm [7] should be considered.) However, any method which searches all 4000 patches for each position of the trajectory is going to be very computer intensive.

2.2 Specular Paths

Whether gradient techniques such as Newton's method are fast or not, they can give important insight into the motion of specular points. Let the current trajectory position ($\mathbf{R}_t$) of figure 2 vary linearly between the two endpoints $\mathbf{R}_{t1}$ and $\mathbf{R}_{t2}$ as

$$\mathbf{R}_t(\Delta) = \Delta\mathbf{R}_{t2} + (1-\Delta)\mathbf{R}_{t1}. \tag{5}$$

For the surface considered here, the distance function $\mathbf{G}(u,v,\Delta)$ is a continuously differentiable function of u, v, and Δ. Suppose the coordinates of a specular point are known for a particular value of Δ and we wish to observe the motion of the specular point as Δ changes. The following argument is a trivial extension of that given by Longuet-Higgins for a time-varying analytic surface [8]. The conditions for a specular point are given by equations (2) and (3). Taking the differential of equations (2) and (3) with respect to u, v, and Δ yields

$$\frac{\partial^2 \|\mathbf{G}(u,v,\Delta)\|^2}{\partial u^2}du + \frac{\partial^2 \|\mathbf{G}(u,v,\Delta)\|^2}{\partial u \partial v}dv + \frac{\partial^2 \|\mathbf{G}(u,v,\Delta)\|^2}{\partial u \partial \Delta}d\Delta = 0,$$

$$\frac{\partial^2 \|\mathbf{G}(u,v,\Delta)\|^2}{\partial u \partial v}du + \frac{\partial^2 \|\mathbf{G}(u,v,\Delta)\|^2}{\partial v^2}dv + \frac{\partial^2 \|\mathbf{G}(u,v,\Delta)\|^2}{\partial v \partial \Delta}d\Delta = 0,$$

which may be rewritten in matrix form as

$$\mathbf{J}(u,v,\Delta)\begin{bmatrix} du/d\Delta \\ dv/d\Delta \end{bmatrix} = \begin{bmatrix} \frac{\partial^2 \|\mathbf{G}(u,v,\Delta)\|^2}{\partial u \partial \Delta} \\ \frac{\partial^2 \|\mathbf{G}(u,v,\Delta)\|^2}{\partial v \partial \Delta} \end{bmatrix}, \tag{6}$$

where $\mathbf{J}(u,v,\Delta)$ is the same 2×2 Jacobian used in the Newton's method search (with its dependence on Δ explicitly noted). Since the elements of $\mathbf{J}(u,v,\Delta)$ are continuous functions of u, v, and Δ, if $\mathbf{J}(u,v,\Delta)$ is nonsingular, $du/d\Delta$ and $dv/d\Delta$ will both be finite, which implies that the changes in u and v can be kept as small as desired by choosing the change in Δ small enough. Longuet-Higgins [8] refers to the vanishing of the determinant of $\mathbf{J}(u,v,\Delta)$ as a twinkle. The physical significance of this result is that as the source/receiver moves

across a second-order continuous surface, specular points cannot suddenly appear or disappear unless $\mathbf{J}(u, v, \Delta)$ is locally singular. The observation that specular points move in continuous paths broken only when $\mathbf{J}(u, v, \Delta)$ is singular leads directly to the following conclusion. If, for any given trajectory, it were possible to determine all the points (u, v, Δ) for which $\mathbf{J}(u, v, \Delta)$ is singular, it would no longer be necessary to search the entire surface for specular points at different positions along the trajectory. It would only be necessary to find all the specular points corresponding to one trajectory position ($\mathbf{R}_{t1}$ for example) and then track their motion, picking up or losing specular paths only at twinkles. It is shown in section 2.4 that the annihilation or creation of specular paths must also occur in pairs; that is, a pair of specular paths must run into each other to be annihilated, or originate from a single point on the surface to be created.

To get a feel for the potential computational savings to be gained by first finding the twinkles associated with a particular trajectory, consider the previous example. Suppose that on the average there were 10 specular points on our surface of 4000 B-spline patches and that it took about the same amount of time to update the location of 5 specular points as it did to search an entire patch for specular points. Once all the twinkles have been found for the trajectory and the problem is reduced to a specular tracking problem, it will take on the average 1/2000 times as long to find each new set of specular points; thus, the computational time will be reduced from a little over 4-1/2 days to 3-1/3 minutes, plus whatever time it takes to find the twinkles. Recalling that the search for twinkles is only conducted once for a given trajectory, we could reduce the computational time required to simulate the backscatter from complex targets by two or more orders of magnitude.

The following example both clarifies how twinkles may be used to trace the motion of specular points along a surface for a given trajectory, and motivates the derivations that follow. Figures 3 through 8 show the evolution of a specular plot for a simple target surface and an associated trajectory of interest. To keep the example relatively uncluttered, it is assumed that in addition to having the continuity properties discussed before, the surface is such that no specular points lie on its edge for any location along the trajectory. The first step is to find all the specular points associated with the beginning of the trajectory; in this example, only one such point exists on the surface, as shown by the X in figure 3. The next step is to find all the twinkles associated with the chosen trajectory and partition the trajectory ac-

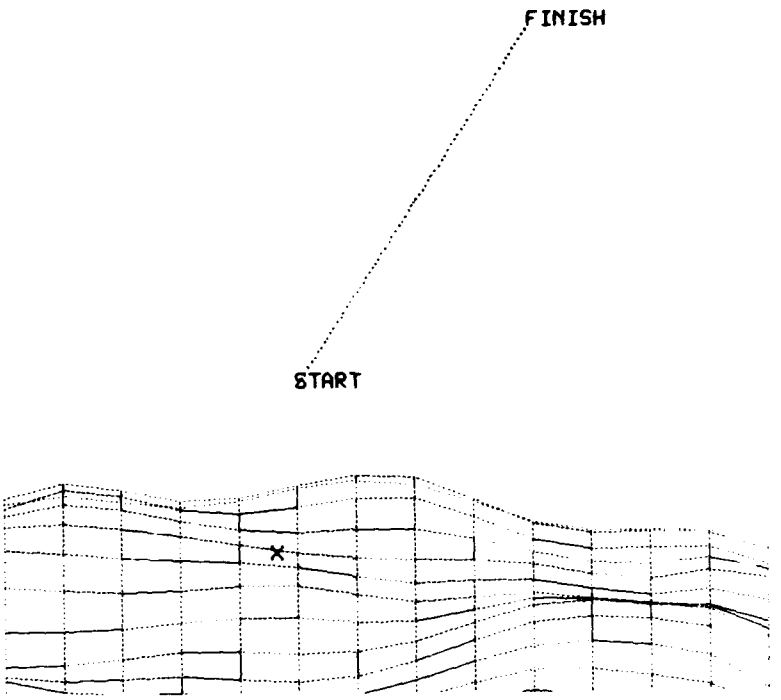

Figure 3: Initial specular point.

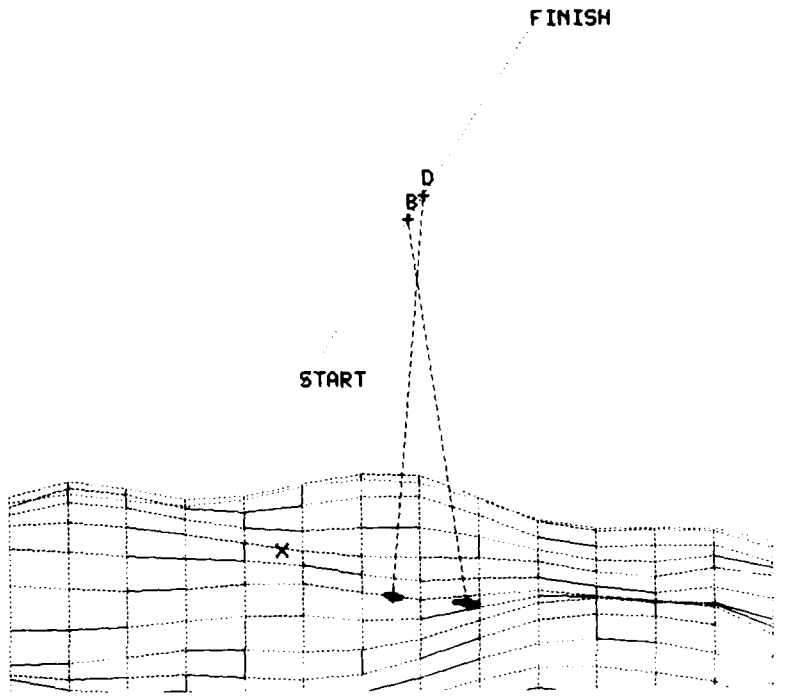

Figure 4: Trajectory partitioned by twinkles.

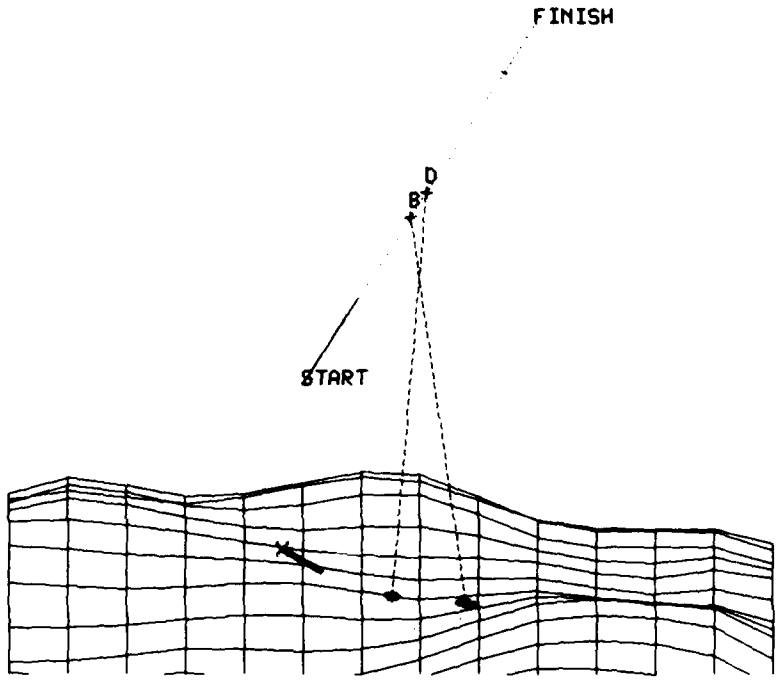

Figure 5: Tracking the initial specular point.

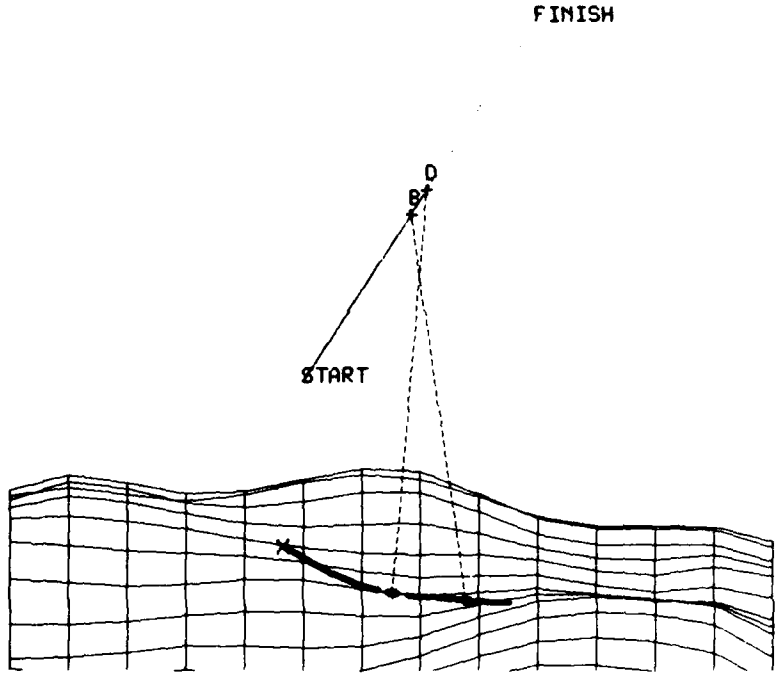

Figure 6: After birth of two specular paths.

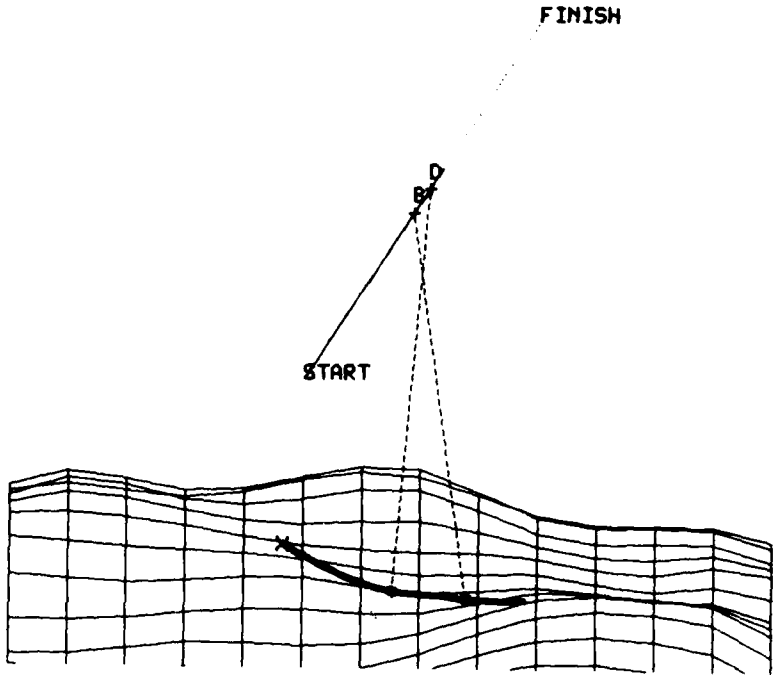

Figure 7: After annihilation of two specular paths.

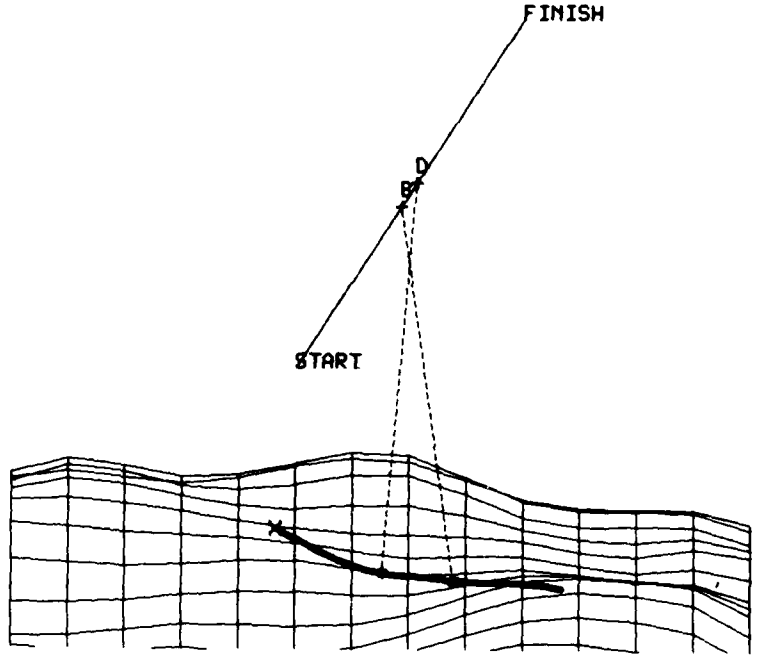

Figure 8: Final specular plot.

cordingly. In addition it will be helpful to know whether each of the twinkles represents a birth or a death of a pair of specular paths. It has already been shown that at a twinkle the Jacobian which might ordinarily be used to determine the location of the specular points becomes singular, making it difficult to locate specular paths near a twinkle. Fortunately, a solution is available to the problem of predicting the motion of specular points near a twinkle, as well as predicting whether a twinkle represents the birth or death of a pair of specular paths, as shown in section 2.4. Figure 4 shows the partitioning of the trajectory, labeling of the twinkles according to whether they represent births or deaths, and prediction of specular paths near the twinkles. For all trajectory locations between the origin of the trajectory and the first twinkle, it is only necessary to determine the motion of the original specular point (since no new specular points will occur anywhere on the surface except at a twinkle). Figure 5 shows the motion of the original specular point in the region preceding the first twinkle. When a twinkle representing the birth of two specular paths is reached, the two new paths must be included in the set of specular points to be tracked, at least until the next twinkle. Figure 6 shows the situation after the first twinkle and shortly before the second. At that time one of the specular points which originated at the birthing twinkle was heading for an annihilation with the original specular point. Figure 7 shows the specular plot at a time after the two specular paths collided at the remaining twinkle. For the remainder of the trajectory, it is only necessary to track the motion of the one remaining specular path, as shown in figure 8. Once again, it should be pointed out that the 14 by 14 grid of spline patches which formed the surface in this example was only searched once for the initial specular points and then once again for the twinkles. After that, specular points were simply tracked.

2.3 Finding Twinkles

As shown in the previous section, a necessary condition for the creation or annihilation of a specular path is the vanishing of the determinant of $\mathbf{J}(u, v, \Delta)$. Denote the determinant of $\mathbf{J}(u, v, \Delta)$ as $F_3(u, v, \Delta)$. Then $F_3(u, v, \Delta)$ is given by

$$F_3(u,v,\Delta) = \frac{\partial^2 \mathbf{G}(u,v,\Delta)}{\partial u^2} \frac{\partial^2 \mathbf{G}(u,v,\Delta)}{\partial v^2} - \left(\frac{\partial^2 \mathbf{G}(u,v,\Delta)}{\partial u \partial v} \right)^2 . \quad (7)$$

In addition to $F_3(u,v,\Delta)$ vanishing, the conditions of a specular point must still be satisfied in order for the point (u,v,Δ) to be a twinkle. Given a target surface and a particular trajectory of interest, the twinkles for the trajectory may be found by solving the nonlinear equations

$$F_1(u,v,\Delta) = 0, \tag{8}$$

$$F_2(u,v,\Delta) = 0, \tag{9}$$

$$F_3(u,v,\Delta) = 0, \tag{10}$$

for the three unknowns u, v, and Δ. Once again, simple gradient techniques may be used to search for the solutions of (8)–(10). The actual Newton steps for finding the twinkle coordinates u, v, and Δ on a uniform B-spline mesh are derived in appendix B.

2.4 Birthing Specular Paths

By themselves, the conditions for a twinkle do not tell whether a particular twinkle represents a birth or death of a pair of specular points with respect to a chosen positive trajectory direction. Once again, a straightforward extension of the analysis by Longuet-Higgins [8] gives a method for describing the motion of specular paths near a twinkle, including whether the twinkle represents the birth or death of a pair of paths. Consider the following substitutions in Longuet-Higgins analysis for the motion of specular points near a twinkle:

$$\begin{aligned} x &:= u, \\ y &:= v, \\ t &:= \Delta, \\ f(x,y,t) &:= \|\mathbf{G}(u,v,\Delta)\|^2, \\ a_{ijk} &= \left.\frac{\partial^{i+j+k}\|\mathbf{G}(u,v,\Delta)\|^2}{\partial u^i \partial v^j 7 \partial \Delta^k}\right|_{u=v=\Delta=0}, \end{aligned}$$

where the coordinate system is chosen such that $u = v = \Delta = 0$ at the twinkle and

$$a_{000} = a_{100} = a_{010} = a_{110} = a_{200} = 0. \tag{11}$$

It can be easily seen from Longuet-Higgins analysis that near a twinkle the u, v coordinates of a specular point are given by

$$\begin{aligned} u &= \pm\left[\frac{-2a_{101}\Delta}{a_{300}}\right]^{1/2}, \\ v &= \frac{a_{210}a_{101} - a_{300}a_{011}}{a_{300}a_{020}}, \end{aligned} \tag{12}$$

Equations (12) show that if a_{101}/a_{300} is positive, then two solutions exist when Δ is less than zero and no solutions exist when Δ is greater than zero; that is, a pair of specular paths is annihilated. Similarly, a pair of specular paths is created when a_{101}/a_{300} is negative. It remains to determine a transformation of coordinates for which equations (12) hold. Simply choosing the origin of the new coordinate system to be the location of the twinkle ensures that a_{000} is equal to zero. It will be useful here and for analysis to come to consider the surface formed by letting the function $\|\mathbf{G}(u,v,\Delta)\|^2$ be the w coordinate in an orthogonal u, v, w coordinate frame, as shown in figure 9. For lack of a better term, this surface is referred to as the "distance surface." The condition for a twinkle may then be interpreted physically as the vanishing of the Gaussian curvature of the distance surface. Or alternately stated, at a twinkle, one of the two principal radii of curvature of the distance surface is equal to zero. The curvature of any smooth surface, at a given point, in the direction δu, δv may be written as (see, among others, Faux and Pratt [9])

$$\kappa_n = (\delta u)^2 a_{200} + (\delta u)(\delta v) a_{110} + (\delta v)^2 a_{020}. \tag{13}$$

Now suppose the coordinates are rotated so that the u-coordinate is aligned with the principal radii of curvature having zero value (such a direction must exist at a twinkle). Then with $\delta v = 0$, equation (13) yields

$$0 = (\delta u)^2 a_{200},$$

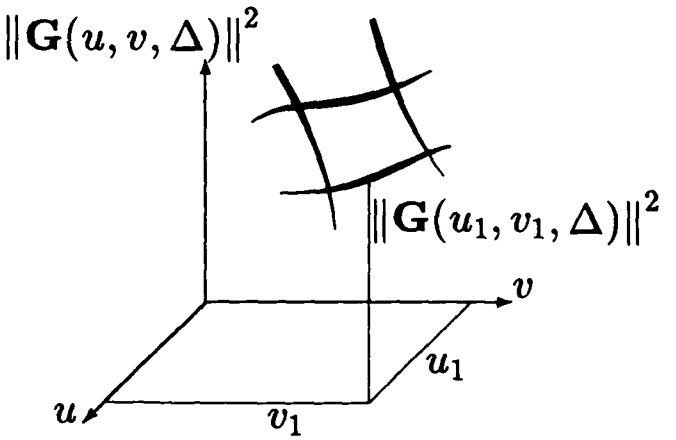

Figure 9: Distance surface.

which implies that $a_{200} = 0$. It can be seen that the twinkle condition implies

$$a_{200}a_{020} - a_{110}^2 = 0.$$

Therefore, in the rotated coordinate system, a_{110} must also be equal to zero and equations (11) are satisfied. Define the new coordinates u', v', and Δ' by

$$\begin{aligned} u &= u' \cos\theta - v' \sin\theta + u_{tw}, \\ v &= u' \sin\theta + v' \cos\theta + v_{tw}, \\ \Delta &= \Delta' + \delta_{tw}, \end{aligned}$$

where u_{tw}, v_{tw}, and Δ_{tw} are the original coordinates of the twinkle. Then if θ is the angle which rotates the original u-axis into the direction of zero curvature, the signs of a_{101} and a_{300}, in the new coordinates, will tell whether the twinkle represents a birth or a death. In addition, the motion of the specular points near the twinkle (in the new coordinates) will be given by (12). The derivation of the equations for a_{300}, a_{101}, a_{210}, a_{011}, and a_{020} in terms of the original coordinates and θ is given in appendix C.

2.5 Rotation of Coordinates

In order to carry out the procedure of the preceding section, it is necessary to determine the angle θ which rotates the original u-direction into the direction of zero (principal) radius of curvature. Define $\mathbf{U}(t) := (u(t), v(t))$ to be a curve on the surface $\mathbf{R}(u(t), v(t))$. It can be shown (see for example, Faux and Pratt [9], p 112) that for $d\mathbf{U}/dt$ to be in the direction of a principal radius of curvature it must satisfy the following matrix equation:

$$[\mathbf{D} - \kappa_n \mathbf{E}] d\mathbf{U}/dt = 0$$

where

$$[\mathbf{D}] = \begin{bmatrix} \mathbf{n} \cdot \frac{\partial^2 \mathbf{r}(u,v)}{\partial u^2} & \mathbf{n} \cdot \frac{\partial^2 \mathbf{r}(u,v)}{\partial u \partial v} \\ \mathbf{n} \cdot \frac{\partial^2 \mathbf{r}(u,v)}{\partial u \partial v} & \mathbf{n} \cdot \frac{\partial^2 \mathbf{r}(u,v)}{\partial v^2} \end{bmatrix},$$

$$[\mathbf{E}] = \begin{bmatrix} \frac{\partial \mathbf{r}(u,v)}{\partial u} \cdot \frac{\partial \mathbf{r}(u,v)}{\partial u} & \frac{\partial \mathbf{r}(u,v)}{\partial u} \cdot \frac{\partial \mathbf{r}(u,v)}{\partial v} \\ \frac{\partial \mathbf{r}(u,v)}{\partial u} \cdot \frac{\partial \mathbf{r}(u,v)}{\partial v} & \frac{\partial \mathbf{r}(u,v)}{\partial v} \cdot \frac{\partial \mathbf{r}(u,v)}{\partial v} \end{bmatrix},$$

and $\mathbf{n}$ is the local unit normal to the surface. The conditions that $d\mathbf{U}/dt$ point in the direction of a principal radius of curvature and that the curvature be zero require that

$$[\mathbf{D}] d\mathbf{U}/dt = 0. \tag{14}$$

Ordinarily matrix equation (14) would have only the trivial solution $d\mathbf{U}/dt = 0$. However, for the case being considered here, the elements of [D] are the same as the elements of the Jacobian introduced earlier, which has been shown to vanish at a twinkle. Therefore, the two equations implied by (14) are not independent, and we are free to choose either as the necessary condition for $d\mathbf{U}/dt$ to point in the direction of zero curvature. The resulting relation is

$$\dot{u}/\dot{v} = -d_{12}/d_{11}$$

or

$$\theta = \tan^{-1}(-d_{11}/d_{12})$$

where θ is shown in figure 10 and d_{ij} is the i,jth element of [D]. Note that it does not matter in which of the two directions of zero curvature we choose to rotate the u-axis, since specular points will be annihilated or created in both directions.

Once a twinkle is found, it is a straightforward matter then to calculate the angle θ which rotates the original u-axis into the direction of zero (principal) radius of curvature, using the first row of the Jacobian. The equations derived in appendix B can then be used to find the values of a_{300}, a_{101}, a_{210}, a_{011}, and a_{020} in the new coordinate system. Comparison of the signs of a_{300} and a_{101} tells whether the associated twinkle represents a birth or a death of two specular paths. In addition, equations (12) can be used to approximate the motion of the specular points near the twinkle. The approximation can be important in the actual implementation of any algorithms, since the vanishing of the Jacobian at the twinkle makes it difficult to use ordinary gradient techniques to search for the new specular paths indicated by a birth twinkle.

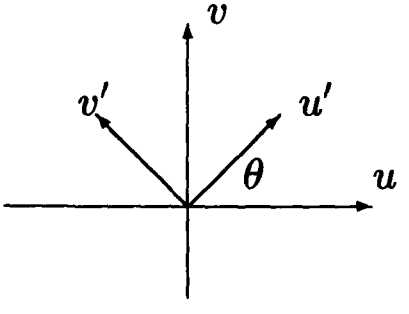

Figure 10: Rotation angle for zero curvature.

3. Extension to Multiple Bounces

3.1 *n*th Order Specular Points

Often multiple-bounce return, as depicted in figure 11, produces a significant contribution to the overall target backscatter. Recall that the geometric optics approach assumes that the energy emanating from the source strikes the target and is then reflected in the same way as would a plane wave incident on a plane tangent to the surface, or put even more intuitively, as a ball bouncing off a billiard cushion. For the single-bounce return already considered, this implies that energy will only return from locations on the surface for which the local surface normal points towards the S/R. However, for complex surfaces, that energy which is reflected by the surface in other directions may strike another surface location so as to be directed back to the receiver. When the magnitude of the energy returned after multiple bounces is calculated, both the increased distance traveled and the loss at each reflection serve to diminish the result. For this reason, the single-bounce return is often referred to as the primary or first-order specular return, while the double-bounce return is referred to as the secondary or second-order specular return (with the obvious notational extension to higher order bounces). The actual target surface locations at which the reflections are considered to occur are denoted the *n*th order specular points. For many targets of interest, it may be assumed that the multiple-bounce return is negligible compared to the single-bounce return. However, if the target surface is assumed to be highly reflective, the local curvatures of the surfaces at the specular

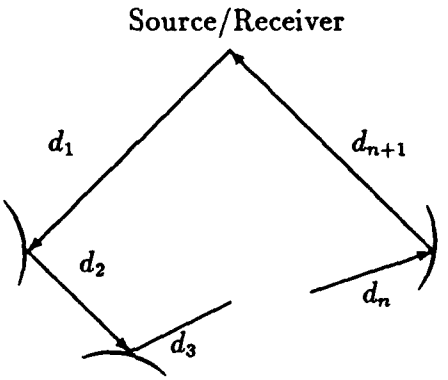

Figure 11: Multiple-bounce return.

points small, and the added round trip distance not too large, then multiple bounces may occur which have return energy with magnitude of the same order as the single bounces.

3.2 The Bistatic Bounce

Fortunately, it can be easily shown that the conditions for an nth order specular bounce are directly related to the total distance of the line segments connecting the source to the receiver via each of the nth order specular points. In fact, the following result can be stated as an immediate consequence of a weak form of Fermat's principle of optics. However, a simple derivation is included here in hopes of giving the reader an intuitive feel for the stationary conditions of the multiple-bounce problem. Consider the case of two rays originating from a point O on an arbitrary surface $(x, y, f(x,y))$, as shown in figure 12. Choose the points A at (x_1, y_1, z_1) and B at (x_2, y_2, z_2) to be points on the two different rays so that the distance $\overline{AO}$ equals the distance $\overline{OB}$. Without loss of generality, we may choose the origin of the system to be at the point O. Define a third point C at (ax_2, ay_2, az_2). By varying a, notice that the point C can be moved to any position along the ray $\overline{OB}$. The distance $\overline{AOC}$ is given by

$$\begin{aligned} D_{\overline{AOC}} &= \sqrt{(x-x_1)^2+(y-y_1)^2+(f(x,y)-z_1)^2} \\ &+ \sqrt{(x-ax_2)^2+(y-ay_2)^2+(f(x,y)-az_2)^2} \end{aligned}$$

with

$$\begin{aligned} \frac{\partial D}{\partial x} &= 1/D_{\overline{AO}}\left[2(x-x_1)+2(f(x,y)-z_1)\frac{\partial f(x,y)}{\partial x}\right] \\ &+ 1/D_{\overline{OC}}\left[2(x-ax_2)+2(f(x,y)-az_2)\frac{\partial f(x,y)}{\partial x}\right]. \end{aligned}$$

Evaluating the partial derivative at $x = y = f(x,y) = 0$ and setting the result equal to zero yields

$$1/D_{\overline{AO}}\left[x_1 + z_1\frac{\partial f(x,y)}{\partial x}\right] + a/D_{OC}\left[x_2 + z_2\frac{\partial f(x,y)}{\partial x}\right] = 0.$$

Noting that $a/D_{\overline{CO}} = 1/D_{\overline{AO}}$, the condition that the distance $\overline{AOC}$ be stationary with respect to x implies

$$\frac{\partial f(x,y)}{\partial x} = \frac{-(x_1+x_2)}{(z_1+z_2)}. \tag{15}$$

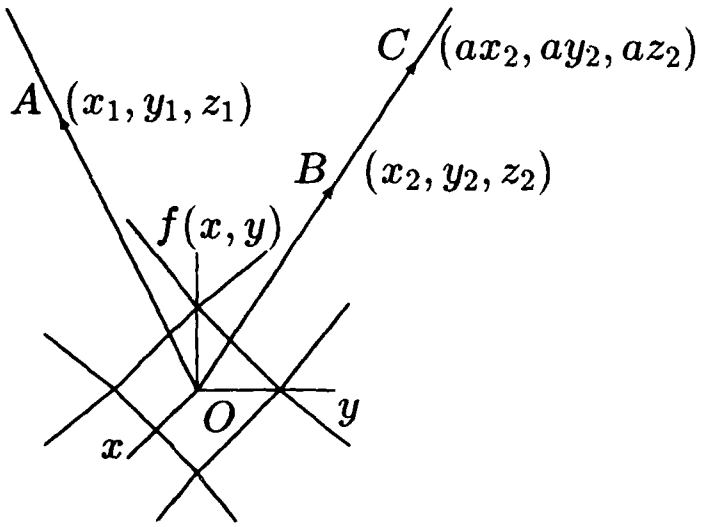

Figure 12: Rays emanating from a surface.

Repeating for the partial derivative of the distance with respect to y yields

$$\frac{\partial f(x,y)}{\partial y} = \frac{-(y_1 + y_2)}{(z_1 + z_2)}. \tag{16}$$

Note that equations (15) and (16) are not defined when $z_1 = -z_2$. However the coordinate system could always be rotated so that z_1 is not equal to z_2, allowing us to assume without loss of generality that z_1 does not equal $-z_2$. Equations (15) and (16) imply that two vectors lying in the tangent plane are

$$\mathbf{T}_1 = (z_1 + z_2)i - (x_1 + x_2)k$$

and

$$\mathbf{T}_2 = (z_1 + z_2)j - (y_1 + y_2)k.$$

And from the above assumption, $\mathbf{T}_1$ and $\mathbf{T}_2$ form a basis for the tangent plane at O.

Now consider the conditions for a bistatic bounce. A ray leaving point A and striking the surface at O will be reflected through C if and only if it passes through B. Since $D_{\overline{AO}}$ is equal to $D_{\overline{BO}}$, any ray starting at (x_1, y_1, z_1) and striking the surface at O will pass through the point (x_2, y_2, z_2) if and only if the ray $\mathbf{R}_m$ (shown in fig. 13) is nor-

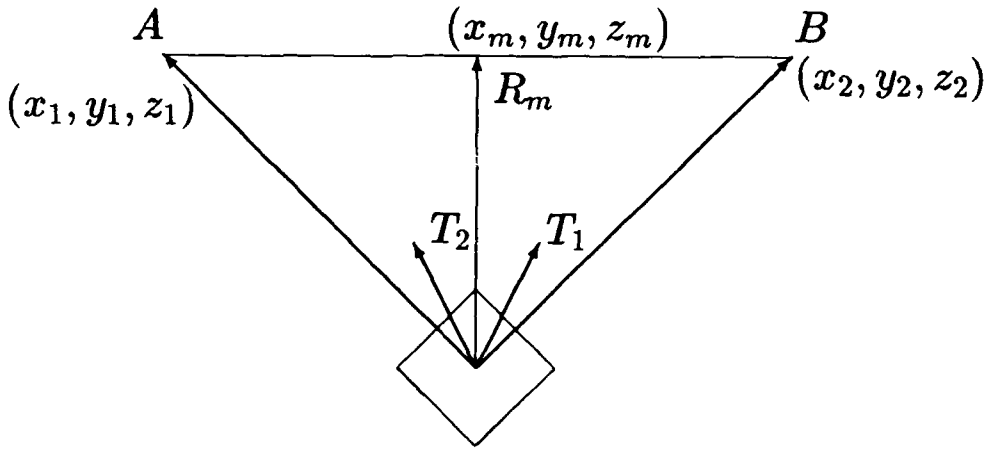

Figure 13: Bistatic bounce.

mal to the surface tangent plane at O. The ray $\mathbf{R}_m$ connects the origin with the point (x_m, y_m, z_m) which lies midway between (x_1, y_1, z_1) and (x_2, y_2, z_2). If $\mathbf{R}_m$ is orthogonal to both $\mathbf{T}_1$ and $\mathbf{T}_2$ as defined above, then $\mathbf{R}_m$ will be normal to the surface tangent plane at O.

$$\mathbf{R}_m = 1/2[(x_1 + x_2)\mathbf{i} + (y_1 + y_2)\mathbf{j} + (z_1 + z_2)\mathbf{k}]$$

implies

$$< \mathbf{R}_m, \mathbf{T}_1 >= 1/2[(x_1 + x_2)(z_1 + z_2) - (x_1 + x_2)(z_1 + z_2)] = 0,$$

$$< \mathbf{R}_m, \mathbf{T}_2 >= 1/2[(y_1 + y_2)(z_1 + z_2) - (y_1 + y_2)(z_1 + z_2)] = 0.$$

Under the mild assumptions that the surface is continuous and differentiable with respect to both x and y, if the distance A to O to C is stationary with respect to the surface parameters at O, then the conditions for a bistatic bounce are satisfied.

3.3 The nth Order Bounce

Consider the implications of the previous bistatic result for a double bounce. The double bounce (in which a signal originates at 1, is bounced from 2 to 3, and then from 3 to 1, as shown in fig. 14) may

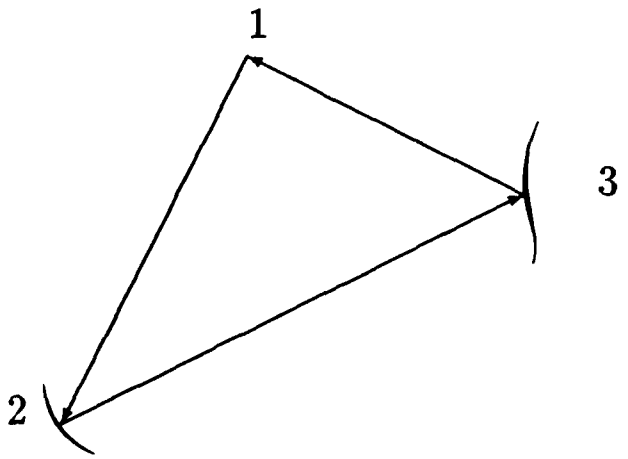

Figure 14: Double bounce.

be viewed as the simultaneous result of two bistatic return problems: i.e., from 1 to 2 to 3 and from 2 to 3 to 1. Both of the bistatic cases must satisfy their respective local stationary conditions, and so the total distance $\overline{12} + \overline{23} + \overline{31}$ must be stationary with respect to the four surface parameters used to describe the two reflecting surfaces. The argument immediately generalizes to any number of bounces. Thus, just as the single-bounce specular points on a surface may be found by searching for stationary points of the distance from the source/receiver to the surface (and back if you like), multiple-bounce paths may be found by searching for stationary points of the total round-trip distance. Each new bounce simply introduces two new stationary conditions along with two new surface parameters. The same Newton technique which was used to find single-bounce specular points may be used to find multiple-bounce specular points (recall that we are ignoring for now the problem of shadowing). The stationary conditions may be stated in terms of the distances shown in figure 11 as

$$\frac{\partial \sum_{i=1}^{n} d_i}{\partial u_j} = 0 = \frac{\partial \sum_{i=1}^{n} d_i}{\partial v_j}$$

for all $j = 1, ..., n$. Noting that

$$\frac{\partial d_i}{\partial u_j} = \frac{\partial d_i}{\partial v_j} = 0$$

whenever $i-1 \leq j$ or $j \geq i+2$, we get the $2n$ conditions

$$\frac{\partial(d_i + d_{i+1})}{\partial u_i} = 0 = \frac{\partial(d_i + d_{i+1})}{\partial v_i}.$$

Denote $d_i + d_{i+1}$ by G_i. Then, taking the differential of the previous $2n$ equations with respect to the $2n$ surface parameters $(u_i, v_i, i = 1, n)$ and the trajectory parameter Δ yields

$$\begin{pmatrix} \frac{\partial^2 G_1}{\partial u_1^2} & \frac{\partial^2 G_1}{\partial u_1 \partial v_1} & \cdots & \frac{\partial^2 G_1}{\partial u_1 \partial u_n} & \frac{\partial^2 G_1}{\partial u_1 \partial v_n} \\ \frac{\partial^2 G_2}{\partial u_1 \partial v_1} & \frac{\partial^2 G_2}{\partial v_1^2} & \cdots & \frac{\partial^2 G_2}{\partial u_n \partial v_1} & \frac{\partial^2 G_2}{\partial v_1 \partial v_n} \\ \cdot & \cdot & \cdots & \cdot & \cdot \\ \cdot & \cdot & \cdots & \cdot & \cdot \\ \cdot & \cdot & \cdots & \cdot & \cdot \\ \frac{\partial^2 G_n}{\partial u_1 \partial v_n} & \frac{\partial^2 G_n}{\partial v_1 \partial v_n} & \cdots & \frac{\partial^2 G_n}{\partial u_n \partial v_n} & \frac{\partial^2 G_n}{\partial v_n^2} \end{pmatrix} \begin{bmatrix} \frac{du_1}{d\Delta} \\ \frac{dv_1}{d\Delta} \\ \cdot \\ \cdot \\ \cdot \\ \frac{dv_n}{d\Delta} \end{bmatrix} = \begin{bmatrix} -\frac{\partial^2 G_1}{\partial u_1 \partial \Delta} \\ -\frac{\partial^2 G_2}{\partial v_1 \partial \Delta} \\ \cdot \\ \cdot \\ \cdot \\ -\frac{\partial^2 G_2}{\partial v_n \partial \Delta} \end{bmatrix}. \tag{17}$$

The same argument that led to the conclusion that specular paths can only be created or annihilated at twinkles may be directly extended to include multiple-bounce twinkles; i.e., the vanishing of the determinant of the $2n \times 2n$ Jacobian of equation (17) is required for a discontinuous motion of the nth order specular paths.

3.4 Example of Savings Using Multiple-Bounce Twinkles

Consider again a B-spline surface made up of 4000 patches: now consider the computational time required to compute the second-order (double-bounce) return from the target. The search for second-order specular points may be conducted by checking all pairs of patches for the stationary conditions described earlier. If we know that a ray leaving the source strikes the ith patch, then strikes the jth patch, and finally returns to the receiver, there is no need to search for a ray leaving the source, striking the jth surface and then the ith surface, and then returning to the receiver. Note however, that it may be possible for a multiple bounce to occur on a single patch. The number of patch combinations which must be considered for each location along the trajectory is therefore simply the number of distinct combinations of the patches taken n at a time, where n is the number of bounces. The number of distinct patch combinations which must be considered, given k patches and n bounces, is simply

$$C = \left(\frac{k!}{n!(k-n)!} \right).$$

For $k >> n$ the number of patch combinations is closely approximated by

$$C \cong \frac{k^n}{n!}.$$

Once again, suppose that there are on the average 10 double-bounce specular paths (20 double-bounce specular points) on the surface for any single location along a given trajectory, and that it takes about the same amount of time to update the location of 5 paths as it does to search an entire pair of patches for an unknown number of double-bounce paths. Once all the double-bounce twinkles have been found for the trajectory and the problem is reduced to a specular tracking problem, it will take on the average 4×10^7 times as long to search the entire target surface for double-bounce specular paths as it will to track the paths. More generally, let T_m denote the average time required to update the n-bounce specular paths and T_s be the average time required to search an n-patch combination for an unknown number of specular points. Then, once the twinkles and initial n-bounce specular paths have been found, it will take Q times as long to search the entire surface for specular paths as it will to update the paths, where Q is given by

$$Q \cong \frac{(T_s)k^n}{(T_m)n!}.$$

Of course, it would be hoped that a one-time search of the surface for patch combinations that could not be involved in a multiple bounce for any trajectory would drastically reduce the number of patches to consider. However, on a complex surface, the number of potential multiple-bounce patch combinations is still likely to be very large and it is clearly worth spending some time searching for the multiple-bounce twinkles.

4. Algorithm Development and Examples

4.1 Introduction

The flow of programs required to implement the twinkle method is outlined in this section, and examples of the results of some simple Fortran 77 realizations of these algorithms are given. The simple programs make the (occasionally incorrect) assumption that at most one twinkle and/or initial specular point will be present on a single B-spline patch. In addition to examples where the simple programs work without a hitch, some examples are discussed to show the effects of missing either a twinkle or an initial specular point. It is also shown that in many cases the results of tracking the specular paths can lead to discovering twinkles that were initially missed.

4.2 Program Flow

Figure 15 is a flow chart of a simplistic program which finds the motion of single-bounce specular points along the target surface as the S/R moves along the trajectory. Once the desired B-spline target surface and trajectory have been selected, the search for twinkles and initial specular points begins. The method used to search for twinkles is simply to start at the center of each patch and the center of the trajectory, and then make the Newton step derived in appendix B. If the steps are such that the search is led off the patch or trajectory, the search is resumed at the appropriate edge. If the search continues to leave the patch or trajectory, it is assumed that the patch has no twinkles for the given trajectory. Such an approach will never find more than one twinkle on a single patch and is not even guaranteed to converge to a twinkle if it is the only one on the patch. However, the method is adequate for the purposes of demonstrating the overall simulation technique and is fairly robust. For example, when the patches are small compared to the overall target, most trajectories are such that no single patch has more than one twinkle. In addition, when a single twinkle does exist on a patch, the method nearly always converges to the twinkle. The terms "nearly always," "small," and "most" are used very loosely in this discussion and are meant only to convey the message that even when such a simplistic technique for searching for the twinkles is used, the method often works. When a twinkle is found, the analysis of sections 2.4 and 2.5 is used to calculate the coefficients of the Taylor series expansion of the motion of the specular points near the twinkle, as well as to determine whether

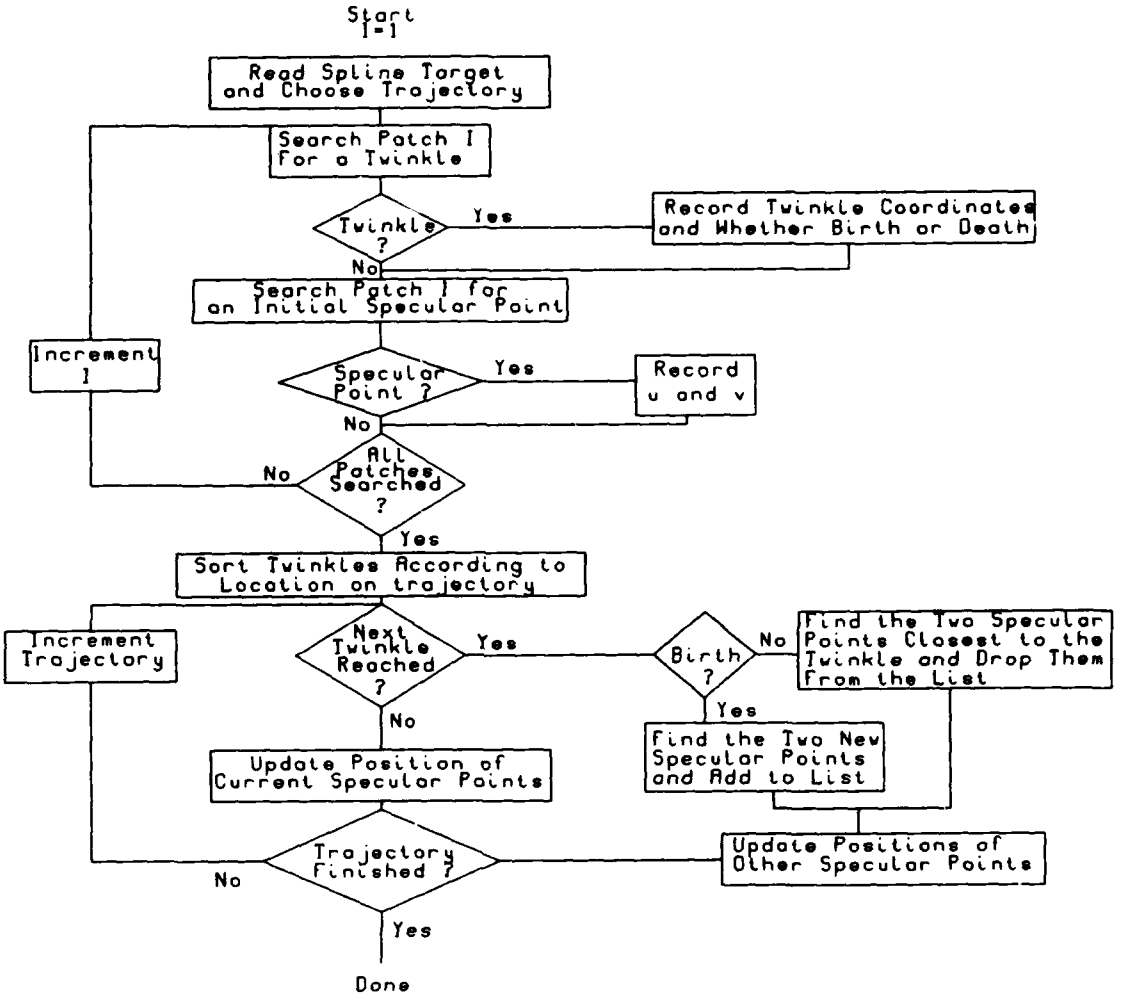

Figure 15: Simple flow chart of algorithm for tracking specular points.

the twinkle represents the birth or death of a pair of specular tracks.

The search for the specular points associated with the beginning of the trajectory is conducted in a manner analogous to the search for twinkles. For each patch, the initial guess for the location of a specular point relative to the trajectory origin is at the center of the patch. If the search exceeds some criterion for leaving the patch, it is assumed that no specular points exist on the patch at the beginning of the trajectory. If a specular point is found, it is assumed to be the only one on that patch.

Once the twinkles and initial specular points are found, it is a simple matter to sort the twinkles according to their trajectory position. With the assurance that no new specular paths will be created before the next twinkle is reached, tracking the motion of the specular points becomes very fast. The current program simply uses the last known location of each specular point as the starting point for a Newton search. The search for each updated position generally takes only a few steps to converge. When the next twinkle is reached, the action to be taken of course depends on whether the twinkle was found to be a creation or annihilation. For an annihilation, a check of the distances from the twinkle to each of the specular points quickly shows which two specular points are colliding. The two points which are closest to the twinkle are simply dropped from the list of specular points to be tracked. If the twinkle represents a creation, then the Taylor coefficients for the motion of the specular points near the twinkle are used to find the locations of the two new specular paths shortly after the twinkle.

4.3 Another Single-Bounce Example

Figures 16 and 17 show another more complex example of the use of twinkles for tracking single-bounce specular paths on a B-spline surface. Figure 16 shows the B-spline surface control mesh and desired trajectory, as well as the locations along the trajectory where specular path discontinuities are expected (based on a search for twinkles). Each twinkle location along the trajectory is labeled B or D, depending on whether the twinkle represents the birth or death of a pair of specular paths, and lines have been drawn connecting them with their associated locations on the target surface. In addition, the predicted paths of the specular points in the area near each twinkle are shown. Figure 17 shows the results after tracking the specular paths for 1000 locations along the trajectory. A comparison of figures 16 and 17

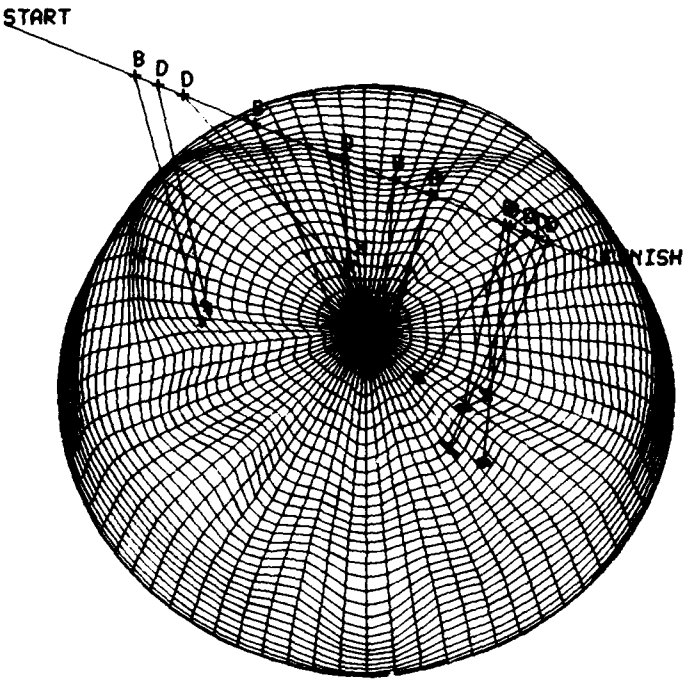

Figure 16: Twinkles and initial specular points.

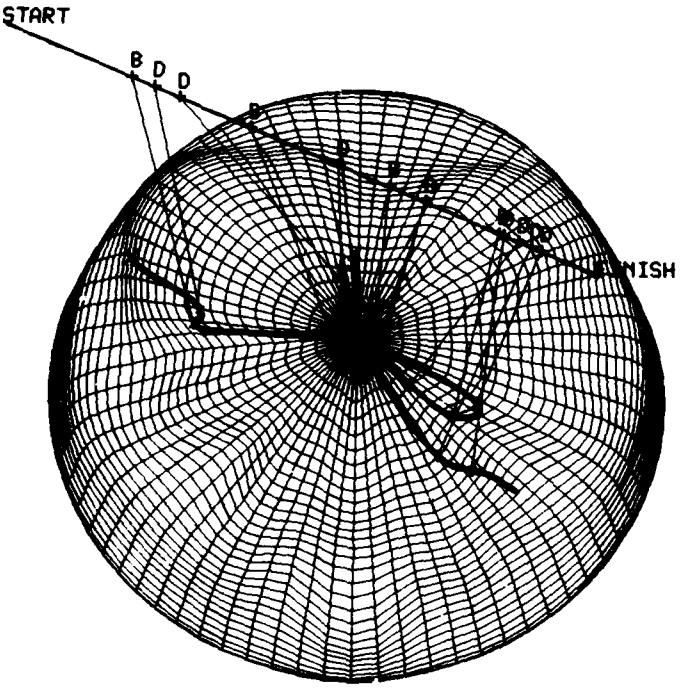

Figure 17: Specular point paths.

shows that the specular paths did in fact remain continuous everywhere except at the twinkles and moved as predicted in the regions near each twinkle. Because completely searching the entire target for specular points at each trajectory location was unnecessary, the entire simulation took only a couple of minutes. Even if the global search for specular points could be reduced to 10 s per trajectory location, the simulation would have taken over 2-1/2 hours without the use of twinkles.

4.4 Missing a Twinkle

Consider the effect of missing a twinkle representing the death of two specular paths. With no modifications to the flow chart shown in figure 15, the program would continue endlessly searching for the two specular points which would still be presumed to exist after reaching the location of the missed twinkle. However, such a situation (a missing twinkle representing an annihilation) can easily be checked for. A quick calculation would show that near the lost path(s), two specular points were very close together. The program could conclude that a twinkle representing a death had been missed, drop the two specular points from the list to be tracked, and proceed. A missing twinkle which represents the death of two specular paths is therefore easy to handle and causes no great concern to the program. For the case of a finely incremented trajectory, the tracking, creation, and annihilation portions of the current simple program are each efficient and reliable. Experience has shown that if the program cannot update a specular point which is supposed to be there, it invariably turns out that the specular point has been annihilated at a twinkle which was missed in the original search. In fact, twinkles which represent annihilations of specular paths could be considered somewhat redundant checks of the specular search.

Simple questions added to the algorithms can provide feedback which corrects for most missing initial specular points and twinkles. The basic premise is that errors at one stage of the specular tracking will show up as inconsistencies in later annihilations or creations. For example, if a twinkle representing an annihilation is reached which has only one approaching specular path, the Taylor expansion can be used to find the missing path near the twinkle. Once the missing path has been found, the trajectory may be backtracked until the source of the missing path is reached. The source of the missing path may then be tested to see if it resulted from a missed initial specular point

or a twinkle representing a birth. If the original error was a missed birthing twinkle, the program must find and track forward the other specular path which must also have been missed. Such a back-and-forth tracking scheme can be effective in finding and correcting for the occasionally missed twinkle or initial specular point. Note for example, that in the case shown in figures 16 and 17, if any one of the initial specular points or twinkles had been missed, they could have been found and corrected for with the above scheme.

If it were not for the fact that a pair of specular paths may be created which never annihilate with any other paths for a particular trajectory, it might be possible to skip the search for twinkles altogether. However, those pairs of paths that were created at a twinkle and either annihilated with each other later or never annihilated at all would not be found under such a scheme. It should also be pointed out that the use of feedback to search for missing twinkles or initial specular paths requires a history of all the specular paths to be kept, so that the formerly lost paths may be added in appropriately. Note that if no initial specular points or twinkles are missed, then the simulated backscatter may be calculated at each step and there is no need to record the actual paths. Fortran implementations of the feedback strategy have been successfully developed. However, while feedback may be used to correct for most missing twinkles and initial specular points, it is still clearly to our advantage to pursue methods which reduce the chances of either.

4.5 Double-Bounce Example

Figures 18 and 19 show an example of the use of double-bounce twinkles for tracking double-bounce specular points on a simple B-spline surface. Figure 18 shows a control mesh for a simple crescent-shaped ribbon which has been tilted slightly so it may be viewed. A short trajectory is shown along with the only double-bounce twinkle associated with that trajectory and surface. In addition, a triangle has been drawn to show the double-bounce path associated with the twinkle. Figure 19 shows the results of searching for double-bounce specular points at 40 locations along the trajectory (starting at the lower left of the trajectory). As expected, the number of double-bounce specular points associated with each trajectory location before the twinkle did not change (there were none). At the twinkle, two sets of specular paths were created (pairs of specular bounces associated with the same double-bounce path are shown connected by a line). The two

sets of double-bounce paths moved in generally opposing directions from their origin.

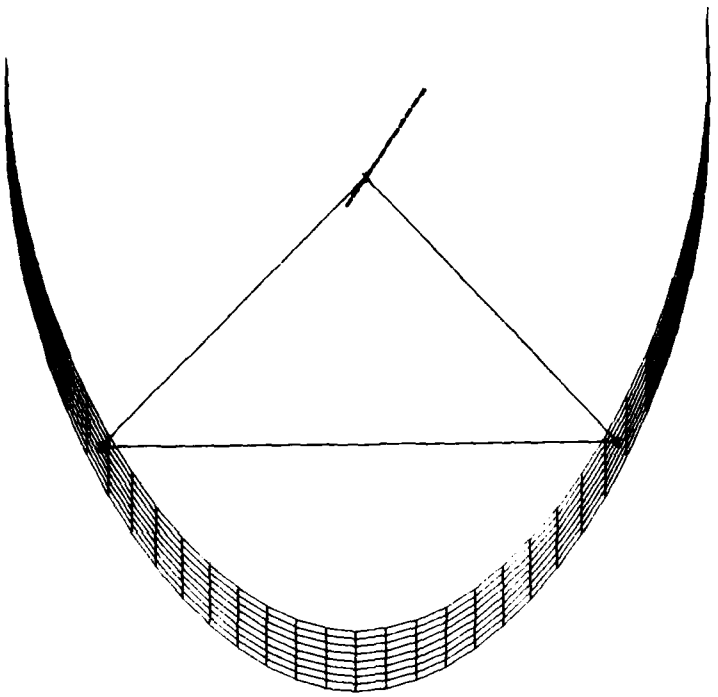

Figure 18: Double-bounce twinkle.

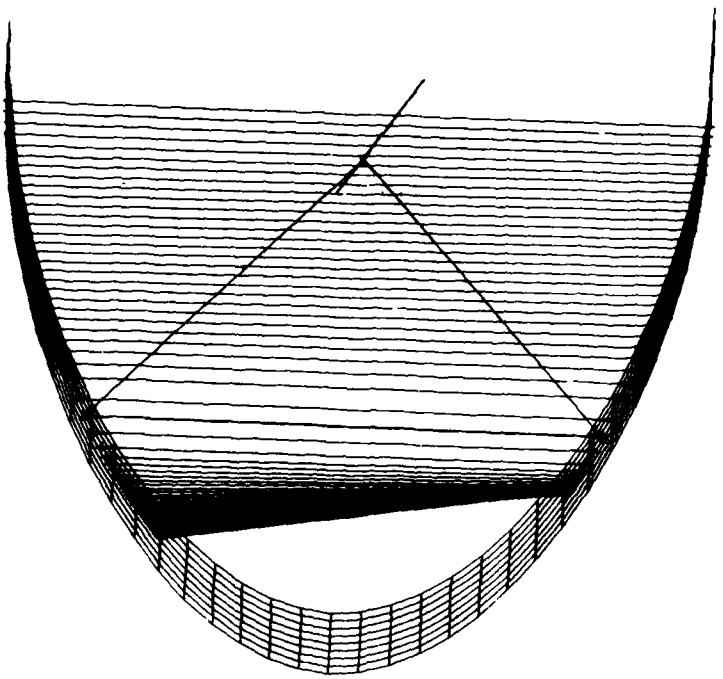

Figure 19: Double-bounce specular point paths.

5. Proposed Additional Research

5.1 Introduction

The use of twinkles to reduce the computational time required for calculating the expected return from complex targets certainly has the potential to be a useful simulation tool. There are of course questions which must be addressed before the technique could be used for most practical applications. Specifically, can practical algorithms be developed which are assured to find all the twinkles and initial specular points for a complex target? What happens if the target surface contains discontinuities or is made up of separate bodies? And what about the effects of shadowing? This section attempts to show that each of these questions can be answered in a positive manner and should be the topics of further research. The section closes with the suggestion that such further research also include experimental validation of the method and comparison with other suitable methods.

5.2 Efficiently Searching for Twinkles and Initial Specular Points

Developing efficient yet thorough algorithms for finding the twinkles and specular points associated with a particular trajectory and its beginning is an important next step in the development of the overall simulation method. Once the twinkles and initial specular points are located, the process of determining the motion of the specular points is both straightforward and efficient. As was pointed out in the previous examples, however, if either a twinkle associated with a birth or an initial specular point is overlooked, it is possible to miss an entire specular path. Thus, the overall simulation method will be no more robust than the method for finding the twinkles and initial specular points. This section begins by showing two fairly obvious methods for reducing the area of the target which must be searched for either twinkles or specular points. A proposal is then made to exploit the variation-diminishing property of B-spline surfaces to develop techniques which partition individual B-spline patches into sections which do not have twinkles or specular points and those which may have.

Regardless of the actual gradient method used to locally search for either twinkles or specular points, it would be profitable to develop techniques which quickly eliminate areas to be searched: i.e., areas for which one of the necessary conditions cannot be met. When the target surface is described by a mesh of B-spline patches, it makes sense to consider the individual patches as identities to be tested.

For example, patches which face in a considerably different direction from that of the trajectory origin can be quickly identified and need not be searched at all when initial specular points are sought. The following is a second and particularly useful technique for eliminating large numbers of patches from the twinkle search.

Recall that if the function $\|\mathbf{G}(u,v,\Delta)\|^2$ is considered to be the w-coordinate in an orthogonal u, v, w coordinate frame as was shown in figure 9, the condition for a twinkle implies that one of the two principal radii of curvature of the newly defined surface is equal to zero. Let u_{tw}, v_{tw}, and Δ_{tw} be the values of u, v, and Δ at a twinkle. Another interpretation is that there exists a curve on the surface passing through u_{tw}, v_{tw} with the radius of curvature originating at the trajectory location, a fraction Δ_{tw} along the trajectory. Clearly, if a particular B-spline patch is totally convex with its radius pointing away from the trajectory, then the surface $(u,v,\|\mathbf{G}(u,v,\Delta)\|^2)$ will also be convex with the radius pointing away from the trajectory. And therefore, the patch cannot contain a twinkle (note that this does not imply that the patch will not have specular points). In most cases a particular B-spline patch is only viewed from one side (for example if the patch is part of a closed surface). Therefore such totally convex patches can be eliminated from the twinkle search for all trajectories of interest. Since many targets consist of large areas of convex cap regions (regions where the curvature does not change sign and points toward the target interior), the savings from the reduced twinkle search can be substantial. This technique is particularly efficient since the patches to be eliminated are found only once for a particular target and their identification stored away for rapid future use with all trajectories.

Now consider the problem which occurs when we attempt to find all the specular points associated with the initial trajectory location. After those patches which are deemed unable to contain any specular points are removed from the search, we are still left with the problem of searching individual patches for an unknown number of specular points. Since specular points may occur arbitrarily close to each other, we would have to begin specular searches arbitrarily close to each other to ensure that all the points are found.

Until now, the second-order continuity of the B-spline surface is the only feature of the surface which has been specifically exploited. However, an important property of B-spline surfaces is their variation-diminishing property. Loosely stated, the variation-diminishing property says that each bicubic B-spline surface patch on a uniform rec-

tilinear mesh will have no more undulations than the 16 three-dimensional data points on which it is defined. As an immediate consequence, if we wanted to find local maxima (minima) on a B-spline target, it would only be necessary to search areas near data points which are themselves local maxima (minima) with respect to neighboring data points. It would be tempting to conclude that in order to find all the locations on the target surface for which the distance to a point on the trajectory is a local maximum (minimum), it is only necessary to search near data points for which the distance to the trajectory is a maximum (minimum) with respect to its neighboring data points. However, such a conclusion would not be valid. To see this, it is only necessary to note that the surface $(u, v, \|\mathbf{G}(u, v, \Delta)\|^2)$ with Δ fixed is a higher order surface than the original B-spline; i.e., the surface is sixth order in both u and v and could clearly have more stationary points than the original bicubic surface. Fortunately, the resulting surface is still just the tensor product of two sixth-order polynomials, and may be represented by the tensor product of two sixth-order B-splines. The resulting higher order B-spline surface patch will be defined by a set of 49 points (7×7 grid) which can then be easily checked for possible maxima (minima). The effort required to transform the distance to the target surface into the higher-order B-spline surface may be considerable. However, ignoring for now the effects of numerical inaccuracies in the computing process, it should be possible, using the transformed surface, to develop ordinary gradient searches which are assured to converge to all the specular points. Since the global search for specular points need only be conducted once for each trajectory, the time required for the surface transformation may be amply rewarded by the increase in robustness of the overall simulation method.

It may of course be possible to create other more efficient methods for assuring that all the initial specular points are found. At the very least, the method described above can serve as a standard for comparison.

The technique of using the variation-diminishing property of B-spline surfaces to ensure that all the specular points corresponding to the initial trajectory location are found may be extended to give a method for ensuring that all the twinkles corresponding to a particular trajectory are found. Consider the following function:

$$M(u, v, \Delta) = F_1^2 + F_2^2 + F_3^2,$$

where F_1, F_2, and F_3 were defined in equations (2), (3), and (7),

respectively. Clearly, $M(u, v, \Delta)$ is greater than or equal to zero for all u, v, and w. In addition, $M(u^*, v^*, \Delta^*)$ equal to zero implies that u^*, v^*, and Δ^* are the parametric coordinates of a twinkle. If we now let $M(u, v, \Delta)$, u, v, and Δ be the orthogonal axes of a four-dimensional hyperspace, then twinkles will occur for values of u, v, and Δ such that the resulting hypersurface equals zero (which also happens to correspond to a local minimum). Analogous to the previous section, it should be possible to represent the resulting hypersurface by a three-way tensor product of appropriately ordered B-splines:

$$M(u, v, \Delta) = \sum_i \sum_j \sum_k \Lambda_{ijk} B_i(u) B_j(v) B_k(\Delta).$$

The variation-diminishing property now shows that twinkles can only occur near the Λ_{ijk} with negative values.

Once again, this observation may or may not lead to the best method for determining the number and locations of the twinkles associated with a particular trajectory. However, it does indicate that such methods do exist and that further research in this area will probably be productive.

5.3 Specular Paths as Roots of Polynomial Surfaces

Consider again the distance surface of figure 9. The problem of finding all the specular points associated with a single location along the trajectory is the same as that of finding all the extrema (maxima and minima) of the surface. If the surface is a piecewise bicubic polynomial surface, as it would be if the original target were a piecewise bicubic B-spline, the specular points are just the simultaneous roots of the surfaces formed by taking the partial derivatives of the distance surface with respect to the two parameters u and v. In this context, twinkles have a simple intuitive interpretation. They are simply the locations at which the imaginary parts of the complex roots go from being nonzero to zero, or vice versa. (If this is not immediately obvious, just consider the fact that any tensor product polynomial surface of a given order has an invariant number of roots, provided we allow the roots to be complex and count multiple roots.) The motion of the S/R across the target surface results in a continuous distortion of the distance surface. As such, we expect that roots of the partial derivatives of the surface should move in continuous paths. It might appear at first that twinkles represent a violation of the continuity of the paths of the roots. However, that is only because in the search

for specular points, we were only interested in the roots with zero imaginary part. Note that the requirement that specular points must be annihilated or created in pairs can be seen in this context as the fact that the roots which have nonzero imaginary parts must occur in complex conjugate pairs.

Consider two methods for tracking specular points by searching for complex values of the u and v (call them $\tilde{u}$ and $\tilde{v}$) parameters which are extrema of the distance surface. The first is a brute-force method. If we think of each of the polynomial B-spline patches as being defined over the entire imaginary plane, then each patch will contain the same number of extrema (of course some of the extrema may be repeated). It should be possible to find all these complex extrema for a single trajectory location and for each patch, then track the motion of these complex points as the S/R moves along the trajectory. Those extrema which have zero imaginary parts will be given the distinction of being specular points. Unfortunately, if the surface consists of thousands of polynomial patches, then even more thousands of complex extrema will have to be tracked for all positions along the trajectory to assure the invariance in the number of extrema.

For a second method, suppose that the polynomial patches were linked together so that not only the composite surface is smooth in the sense we have been considering, but also the complex extrema of the surface are continuous across patches. With such a surface, it would only be necessary to find all the complex extrema with real parts in the range for which we consider the patch to describe the surface: i.e., the real parts of $\tilde{u}$ and $\tilde{v}$ restricted to [0,1]. Then as the S/R moves along the trajectory, the only way that an extremum could enter a new patch is if it leaves a neighboring patch (ignoring for the moment the edges of the composite surface). If the composite surface is closed, finding all the extrema with real parts in [0,1] will result in finding an invariant set of complex extrema which is much reduced from that of the previous brute-force method.

This method has the potential to be extremely powerful and efficient. Once all the complex extrema are found for any location, they may be tracked to the beginning of any desired trajectory and then tracked along the desired trajectory. Note that it would be trivial to include arbitrary nonlinear trajectories. Note also that because the invariant number of extrema need only be determined once for any given target, the methods used to find the extrema can be extremely thorough.

It should be noted that the search for complex roots can be con-

siderably more difficult than the search for strictly real roots. One potentially useful method for finding the complex roots of a B-spline patch would be to find all the roots for a particular patch (with $\tilde{u}$ and $\tilde{v}$ extended to the entire imaginary plane) chosen to simplify the problem. Once all these roots are found, the B-spline coefficients could be modified to the desired B-spline patch while the complex roots are tracked. This method would assure that all the complex roots are found. Since neighboring patches tend to have similar coefficients, it should be natural and efficient to continue to deform patches into neighboring patches while tracking the effect on the roots.

Unfortunately, cubic B-spline surfaces as used in this report do not provide continuity of the complex roots across patches. One would hope that just as raising the order of the spline allows for additional derivative continuity, perhaps the additional freedom of raising the spline order by one could be used to ensure continuity of the complex roots. Because of the very powerful potential of this method, the requirements for complex root continuity of the B-spline composite surface should be investigated.

5.4 Twinkle Search Through Recursive Subdivision

It was pointed out in section 5.2 that if a portion of the surface is such that its maximum and minimum principal radii of curvature both point toward the interior of the surface, then no twinkles can exist on that portion of the surface for any trajectory. Consider a generalization of this technique. Each point on a patch of the B-spline quilt has associated with it two principal radii of curvature (the maximum and minimum radii of curvature). Suppose the maximum and minimum values of the two principal radii of curvature were known for the entire patch. If we add to the two maxima an amount to account for the finite extent of the patch, and subtract from the minima the same amount, the four resulting radii will provide two bounding volumes, one of which must be intersected by the trajectory if a twinkle is to occur on that patch; i.e., each principal radius of curvature will have associated with it a range guaranteed to include its maximum and minimum values over the entire patch. If the trajectory does not pass through either of these two ranges, then the patch cannot contain a twinkle. Now consider what happens if the original patch is subdivided into four subpatches. The maximum and minimum values of the two principal radii of curvature will become closer to the same on each subpatch, decreasing the volume of space which must

be intersected by the trajectory for any of the subpatches to contain a twinkle (the extent of the patch will decrease as well). In the limit as the patch is recursively subdivided, two concentric spheres will be formed, one of which the trajectory must intersect in order for the subpatch to contain a twinkle.

The above method can be turned into a recursive subdivision technique for finding twinkles by adding the requirement that a twinkle must also be a specular point. Using the normal at the center of a patch along with the maximum curvature for the patch, we can calculate a "normal cone" which includes all possible surface normals for the patch. As the patch is subdivided, each cone will become smaller in extent until, in the limit, the cone becomes a line. Twinkles will be assumed to exist only on those subpatches for which the trajectory, normal cone, and space between appropriate concentric curvature spheres all intersect. The subdivision can be carried out until limited by the precision of the computer, at which time the remaining candidate subpatches may be considered the locations of twinkles. Except for twinkles that lie so close together that the difference in their positions cannot be distinguished with the precision of the computer, the recursive subdivision technique should result in finding all the twinkles for a given trajectory. It should be clear to the reader that the normal cone described above could also be used by itself to define a recursive subdivision test for initial specular points.

It should be possible to simplify the search for the maxima and minima of the two principal curvatures on each subpatch by first finding all stationary points of the principal curvatures for each original patch. The extrema of the principal curvatures on all subpatches would either have to be the extrema of the parent patch or lie along the edge of the subpatch, greatly simplifying the search for the maximum and minimum curvatures of each subpatch. Note that the search for the curvature extrema on the original patches would only have to be carried out once for the model since curvature extrema are independent of the chosen trajectory. It may even be possible to find efficient bounds on the maximum and minimum principal curvatures more directly from the original data points by exploiting the properties of the B-spline surface.

5.5 Inclusion of Surface Discontinuities

The surfaces of most targets of interest are not everywhere second-order continuous. This is particularly obvious in manmade targets

which generally have an abundance of corners and edges. While it may be possible to model edges and corners as second-order continuous surfaces containing locations of very small radius of curvature, in many cases the modeling effort will be made much easier if the constraint of second-order continuity everywhere is reduced; that is, if the surface is everywhere second-order continuous except along edges or corners.

At first glance, it might appear that the use of twinkles to reduce the computational time required to simulate the return from complex targets would be of little use when the surface contains discontinuities of either its first or second derivatives; in such a situation, it would be possible for specular paths to begin and end at places other than twinkles. Fortunately, it is easy to see that for all the target surface which is second-order continuous, specular paths can still only be created or destroyed at twinkles. Therefore, once the twinkles and initial specular points are found, the specular paths can still be tracked, as long as for each new trajectory location all the discontinuities are also checked. If the surface discontinuities occur at isolated points (corners) or along curves (edges), the additional search required by the inclusion of discontinuities will be reduced in order. If in addition the discontinuities are restricted to lie on parametric curves running orthogonal to either of the two surface parameters, the problem becomes particularly simple. For example, the surface normal along one edge of a B-spline patch is a function of only one parameter (with proper choice of axes, the other parameter will be fixed at zero). Thus if a discontinuity lies along the edge of a B-spline patch, it should be a straightforward procedure to find any intersections between the surface normal along the edge and the trajectory. The intersections could be thought of as "pseudo-twinkles" since they represent additional points on the surface at which a specular path may begin or end. If it is necessary to include discontinuities along parametric curves which are not orthogonal to either of the two surface parameters, the algebra becomes somewhat more unwieldy. However, it should still be a fairly straightforward task to find the pseudo-twinkles along the curves for an entire trajectory. Thus the inclusion of curvature, slope, or even position discontinuities in the target surface is another topic whose investigation should prove fruitful.

5.6 Multiple Bodies and Shadowing

Backscatter simulation algorithms based on twinkles are just as applicable to multibody targets as they are to single-body targets. Even for multiple bounces, the question of whether the bounces occur on separate bodies or not never enters into the problem. The problem with finding the return from a target made up of separate bodies is that the effect of shadowing becomes more important; i.e., it is more likely that the ray being considered will have passed through part of the target. Recall that the stationary condition for multiple-bounce return shown earlier (which includes the single-bounce case) does not require such an unobstructed path.

Questions related to shadowing are almost always handled by some form of ray tracing. However, the computational savings due to the use of twinkles would be totally eliminated if it were still necessary to ray trace the entire scene just to handle the shadowing. Those specular points which have been found by ignoring potential shadowing we refer to as "potential specular points." Clearly, the problem of determining whether or not a potential specular point is an actual specular point is greatly simplified by knowledge of its position. At most it will be necessary to check only the paths associated with each specular point for intersections with the target surface at each trajectory location to determine the actual "visibility" of the return. It may even be possible to exploit the continuity of the target surface to reduce the computational time required to search for shadowing structures. For example, if the path connecting a multiple-bounce return is to go from being unshadowed to shadowed, some portion of the path must become osculatory with the target surface at some point. And of course the same must hold for a multiple bounce coming out of shadow. Once the potential specular paths have been determined (ignoring potential shadowing), it may be possible to exploit this shadowing constraint to rapidly determine which portions of the paths should be considered actual specular paths for calculating the expected return.

5.7 Experimental Validation and Comparison

The ultimate goal of this study is to develop a useful radar backscatter modeling technique for such targets as tanks, aircraft, and ships. Clearly then an experiment of interest would be to create a spline model which closely resembles the surface of a target of interest, experimentally determine the backscatter signatures of the actual target

for many trajectories, and compare the results with those calculated from the spline surface using a geometric optics approach. While such experiments will eventually determine the bottom-line effectiveness of the modeling approach, an intermediate set of experiments using a target developed to test specific assumptions of the modeling method should also prove to be informative.

Generally speaking, the use of a geometric optics assumption for the return from complex targets is subject to two broad categories of error. The first type of error is due to the surface description not adequately resembling the actual target surface of interest. The second category of error is due to the geometric optics assumptions themselves (i.e., everything else). For a target such as a tank, there are likely to be a number of items which do not fit the geometric assumptions well. Sharp edges, varying surface material properties, or just plain dirt are only a few examples. A useful experiment therefore would be to construct a complex surface which satisfies the geometric optics assumptions to a high degree for an available radar frequency. The surface should then be accurately modeled by B-splines and the actual and simulated returns compared. Comparisons of signatures using various frequencies and trajectories should lead to greater insight into the overall modeling problem as well as into the limits of the geometric optics approach.

Once a geometric optics model is chosen to simulate the return from complex targets, the method used to find the specular points makes no difference in the calculation of the return (provided each method finds all the specular points for each location of the trajectory). However, the ability to rapidly find all the specular points as a function of the trajectory location does give the ability to conduct a more extensive validation of the model. Such an extensive validation of the model should be performed for a complex but highly controlled target for which the geometric optics assumptions are valid, as well as for actual targets of interest.

6. Summary

Use of the geometric optics approach to simulate the radar backscatter from composite targets can be efficient and informative. The validity of the approach depends on a number of factors, including the target surface characteristics and the wavelength of the propagated signal. The use of B-splines to describe complex targets for use in the geometric optics model is an obvious extension of previous methods. Unfortunately, the increased complexity of the model means an increased search time for a generally unknown number of specular points. Since it is expected that the specular points must be found for thousands of locations along each trajectory, ordinary techniques which search the entire surface for specular points, at each location on the trajectory, are generally too computer intensive to be practical.

Over 25 years ago, Longuet-Higgins [8] pointed out the continuity of specular paths on smooth surfaces and showed the conditions for which a specular path may become discontinuous. It has been shown in this paper that the locations of specular path discontinuities (known as twinkles) may be predicted for an entire trajectory. Once the locations of all the twinkles associated with a particular trajectory are known, it is only necessary to track the motion of specular points as a function of the trajectory location, assured that creations and annihilations of specular paths will only occur at the twinkles. It was shown that the method extends to multiple bounces of any order.

The actual algorithms currently used to find twinkles and initial specular points are implementations of simple local gradient techniques, which offer no assurance of convergence to all the desired points. The shortcomings of these techniques were discussed and suggestions were made for techniques to increase the robustness of the algorithms. In addition, the problems of surface discontinuities and shadowing were briefly discussed, with the conclusion that they may be included in the model without negating the savings incurred by using twinkles. The inclusion of surface discontinuities and shadowing are two more suggested topics of further research.

Consider the problem of simulating the backscatter from a target represented by the equivalent of 10,000 B-spline surface patches for 1000 locations along a specified trajectory. The author anticipates that pursuit of the research suggested in this report will result in algorithms to find the backscatter signatures from such encounters in a matter of minutes, on a reasonably high-powered computer. It should be possible with such a model to capture the significant features of

most complex targets of interest. Such a model would obviously find important applications in many current as well as anticipated projects using high-frequency radar as a source of information.

References

[1] John F. Dammann, *Air Target Models for Fuzing Simulations,* Harry Diamond Laboratories, HDL-TR-1960 (September 1982).

[2] Carl de Boor, *A Practical Guide to Splines,* Springer-Verlag, New York (1978).

[3] William J. Gordon and Richard F. Riesenfeld, *B-Spline Curves and Surfaces,* Proc., Computer Aided Geometric Design Conference, University of Utah, Salt Lake City (18–21 March 1974).

[4] M. G. Cox, *The Numerical Evaluation of B-Splines,* J. Inst. Math. Its Appl. **10** (1972), 134–149.

[5] Donald E. Amos, *Computation with Splines and B-Splines,* Sandia National Laboratory, SAND78-1968 (March 1979).

[6] David G. Luenberger, *Linear and Nonlinear Programming,* Addison-Wesley, Reading, MA (1984).

[7] Elaine Cohen, Tom Lyche, and Richard Riesenfeld, *Discrete B-Splines and Subdivision Techniques in Computer-Aided Geometric Design and Computer Graphics,* Computer Graphics and Image Processing **14** (1980), 87–111.

[8] M. S. Longuet-Higgins, *Reflection and Refraction at a Random Moving Surface. I. Pattern and Paths of Specular Points,* J. Opt. Soc. Am. **50** (1960), 838.

[9] Ivor D. Faux and Michael J. Pratt, *Computational Geometry for Design and Manufacture,* Ellis Horwood, New York, NY (1981).

Appendix A. Newton Step for the Location of a Specular Point on a B-Spline Surface

We are interested in solving the matrix equation

$$\begin{pmatrix} \frac{\partial F_1}{\partial u} & \frac{\partial F_1}{\partial v} \\ \frac{\partial F_2}{\partial u} & \frac{\partial F_2}{\partial v} \end{pmatrix} \begin{bmatrix} S_1 \\ S_2 \end{bmatrix} = \begin{bmatrix} -F_1 \\ -F_2 \end{bmatrix},$$

where

$$F_1 := F_1(u,v,\Delta) = \frac{\partial \|\mathbf{G}(u,v,\Delta)\|^2}{\partial u},$$

$$F_2 := F_2(u,v,\Delta) = \frac{\partial \|\mathbf{G}(u,v,\Delta)\|^2}{\partial v}.$$

If we let the x, y, z coordinates of figure 2 in the body of the report be replaced by X^1, X^2, X^3, respectively, the equation for $\|\mathbf{G}(u,v,\Delta)\|^2$ becomes

$$\|\mathbf{G}(u,v,\Delta)\|^2 = \sum_{i=1}^{3} [\Delta(X_2^i - X_1^i) + X_1^i - R_{x^i}(u,v)]^2$$

where R_{x^i} is the X^i component of the surface $\mathbf{R}(u,v)$. Then,

$$\begin{aligned}
F_1(u,v,\Delta) &= -2\sum_{i=1}^{3} \left\{ [\Delta(X_2^i - X_1^i) + X_1^i - R_{x^i}(u,v)] \frac{\partial R_{x^i}(u,v)}{\partial u} \right\}, \\
F_2(u,v,\Delta) &= -2\sum_{i=1}^{3} \left\{ [\Delta(X_2^i - X_1^i) + X_1^i - R_{x^i}(u,v)] \frac{\partial R_{x^i}(u,v)}{\partial v} \right\}, \\
\frac{\partial F_1(u,v,\Delta)}{\partial u} &= -2\sum_{i=1}^{3} \left\{ [\Delta(X_2^i - X_1^i) + X_1^i - R_{x^i}(u,v)] \frac{\partial^2 R_{x^i}(u,v)}{\partial u^2} \right. \\
&\qquad \left. \left[\frac{\partial R_{x^i}(u,v)}{\partial u} \right]^2 \right\}, \\
\frac{\partial F_2(u,v,\Delta)}{\partial v} &= -2\sum_{i=1}^{3} \left\{ [\Delta(X_2^i - X_1^i) + X_1^i - R_{x^i}(u,v)] \frac{\partial^2 R_{x^i}(u,v)}{\partial v^2} \right. \\
&\qquad \left. \left[\frac{\partial R_{x^i}(u,v)}{\partial v} \right]^2 \right\}, \\
\frac{\partial F_2(u,v,\Delta)}{\partial u} &= -2\sum_{i=1}^{3} \left\{ [\Delta(X_2^i - X_1^i) + X_1^i - R_{x^i}(u,v)] \frac{\partial^2 R_{x^i}(u,v)}{\partial u \partial v} \right. \\
&\qquad \left. \left[\frac{\partial R_{x^i}(u,v)}{\partial u} \frac{\partial R_{x^i}(u,v)}{\partial v} \right] \right\}, \\
\frac{\partial F_1(u,v,\Delta)}{\partial v} &= \frac{\partial F_2(u,v,\Delta)}{\partial u}.
\end{aligned}$$

Appendix A

Let Λ_{ij} be the vector coefficients of a single B-spline patch and denote its x, y, or z component by Λ^k_{ij}. Then for the l,mth patch of the bicubic B-spline surface being considered,

$$R_{lmx^k}(u,v) = \sum_{i=1}^{4}\sum_{j=1}^{4} B_i(u)\Lambda^k_{i+l,j+m}B_j(v),$$

where $B_i(z)$ for i=1, 2, 3, and 4 were given in section 1.3 and $u,v \in [0,1]$. Thus, for any particular patch and trajectory, given u,v, and Δ, the Newton step [S_1,S_2] toward a specular point is given by

$$\begin{bmatrix} S_1 \\ S_2 \end{bmatrix} = \begin{pmatrix} \frac{\partial F_1}{\partial u} & \frac{\partial F_1}{\partial v} \\ \frac{\partial F_2}{\partial u} & \frac{\partial F_2}{\partial v} \end{pmatrix}^{-1} \begin{bmatrix} -F_1 \\ -F_2 \end{bmatrix}.$$

If u,v, and Δ are not the coordinates of a twinkle, then the inverse in the previous equation is guaranteed to exist.

Appendix B. Newton Step for the Location of Twinkles

We are interested in solving the matrix equation

$$\begin{pmatrix} \frac{\partial F_1}{\partial u} & \frac{\partial F_1}{\partial v} & \frac{\partial F_1}{\partial \Delta} \\ \frac{\partial F_2}{\partial u} & \frac{\partial F_2}{\partial v} & \frac{\partial F_2}{\partial \Delta} \\ \frac{\partial F_3}{\partial u} & \frac{\partial F_3}{\partial v} & \frac{\partial F_3}{\partial \Delta} \end{pmatrix} \begin{bmatrix} S_1 \\ S_2 \\ S_3 \end{bmatrix} = \begin{bmatrix} -F_1 \\ -F_2 \\ -F_3 \end{bmatrix},$$

where F_1 and F_2 are the same as in appendix A, and

$$F_3 := F_3(u,v,\Delta) = \frac{\partial F_1(u,v,\Delta)}{\partial u}\frac{\partial F_2(u,v,\Delta)}{\partial v} - \left(\frac{\partial F_1(u,v,\Delta)}{\partial v}\right)^2.$$

Expressions for F_1, F_2, $\frac{\partial F_1}{\partial u}$, $\frac{\partial F_1}{\partial v}$, $\frac{\partial F_2}{\partial u}$, and $\frac{\partial F_2}{\partial v}$ as functions of u, v, and Δ were found in appendix A. Expressions for the remaining terms are as follows:

$$\frac{\partial F_1(u,v,\Delta)}{\partial \Delta} = -2\sum_{i=1}^{3}(X_2^i - X_1^i)\frac{\partial R_{x^i}(u,v)}{\partial u},$$

$$\frac{\partial F_2(u,v,\Delta)}{\partial \Delta} = -2\sum_{i=1}^{3}(X_2^i - X_1^i)\frac{\partial R_{x^i}(u,v)}{\partial v}.$$

Dropping the u, v and Δ arguments for brevity,

$$\begin{aligned}
\frac{\partial F_3}{\partial u} &= \left(\frac{\partial F_1}{\partial u}\right)\left(\frac{\partial^2 F_2}{\partial u \partial v}\right) + \left(\frac{\partial F_2}{\partial v}\right)\left(\frac{\partial^2 F_1}{\partial u^2}\right) - 2\left(\frac{\partial F_1}{\partial v}\right)\left(\frac{\partial^2 F_1}{\partial u \partial v}\right), \\
\frac{\partial F_3}{\partial v} &= \left(\frac{\partial F_1}{\partial u}\right)\left(\frac{\partial^2 F_2}{\partial v^2}\right) + \left(\frac{\partial F_2}{\partial v}\right)\left(\frac{\partial^2 F_1}{\partial u \partial v}\right) - 2\left(\frac{\partial F_1}{\partial v}\right)\left(\frac{\partial^2 F_1}{\partial v^2}\right), \\
\frac{\partial F_3}{\partial \Delta} &= \left(\frac{\partial F_1}{\partial u}\right)\left(\frac{\partial^2 F_2}{\partial \Delta \partial v}\right) + \left(\frac{\partial F_2}{\partial v}\right)\left(\frac{\partial^2 F_1}{\partial \Delta \partial u}\right) - 2\left(\frac{\partial F_1}{\partial v}\right)\left(\frac{\partial^2 F_1}{\partial \Delta \partial v}\right).
\end{aligned}$$

To further abbreviate the notation, let $\psi_i = [\Delta(X_2^i - X_1^i) - X_1^i - R_{x^i}(u,v)]$:

$$\begin{aligned}
\frac{\partial^2 F_2}{\partial u \partial v} &= -2\sum_{i=1}^{3}\left[\psi_i \frac{\partial^3 R_{x^i}(u,v)}{\partial u \partial v^2} - 2\frac{\partial R_{x^i}(u,v)}{\partial v}\frac{\partial^2 R_{x^i}(u,v)}{\partial u \partial v} - \frac{\partial R_{x^i}(u,v)}{\partial u}\frac{\partial^2 R_{x^i}(u,v)}{\partial v^2}\right], \\
\frac{\partial^2 F_1}{\partial u \partial v} &= -2\sum_{i=1}^{3}\left[\psi_i \frac{\partial^3 R_{x^i}(u,v)}{\partial u^2 \partial v} - 2\frac{\partial R_{x^i}(u,v)}{\partial u}\frac{\partial^2 R_{x^i}(u,v)}{\partial u \partial v} - \frac{\partial R_{x^i}(u,v)}{\partial u^2}\frac{\partial^2 R_{x^i}(u,v)}{\partial v}\right], \\
\frac{\partial^2 F_1}{\partial u^2} &= -2\sum_{i=1}^{3}\left[\psi_i \frac{\partial^3 R_{x^i}(u,v)}{\partial u^3} - 3\frac{\partial R_{x^i}(u,v)}{\partial u}\frac{\partial^2 R_{x^i}(u,v)}{\partial u^2}\right],
\end{aligned}$$

Appendix B

$$
\begin{aligned}
\frac{\partial^2 F_2}{\partial v^2} &= -2\sum_{i=1}^{3}\left[\psi_i \frac{\partial^3 R_{x^i}(u,v)}{\partial v^3} - 3\frac{\partial R_{x^i}(u,v)}{\partial v}\frac{\partial^2 R_{x^i}(u,v)}{\partial v^2}\right], \\
\frac{\partial^2 F_2}{\partial \Delta \partial v} &= -2\sum_{i=1}^{3}(X_2^i - X_1^i)\frac{\partial^2 R_{x^i}(u,v)}{\partial v^2}, \\
\frac{\partial^2 F_1}{\partial \Delta \partial u} &= -2\sum_{i=1}^{3}(X_2^i - X_1^i)\frac{\partial^2 R_{x^i}(u,v)}{\partial u^2}, \\
\frac{\partial^2 F_1}{\partial \Delta \partial v} &= -2\sum_{i=1}^{3}(X_2^i - X_1^i)\frac{\partial^2 R_{x^i}(u,v)}{\partial u \partial v}.
\end{aligned}
$$

Appendix C. Taylor Coefficients at a Twinkle in the Rotated Frame

At a twinkle, the Taylor coefficients a_{ijk} are given by

$$a_{ijk} = \left. \frac{\partial^{i+j+k} \|\mathbf{G}(u,v,\Delta)\|^2}{\partial u^i \partial v^j \partial \Delta^k} \right|_{u_{tw}, v_{tw}, \Delta_{tw}}$$

where u_{tw}, v_{tw}, and Δ_{tw} are the coordinates of the twinkle. We are interested in the Taylor coefficients a_{300}, a_{011}, a_{020}, a_{210}, and a_{101} in the u', v', Δ' coordinate system, where

$$u = u' \cos\theta - v' \sin\theta + u_{tw}$$

$$v = u' \sin\theta - v' \cos\theta + v_{tw}.$$

Let Λ_{ij}^k be the scalar components of the vector coefficients of a single B-spline patch, with Λ^k representing the x, y, or z coordinates as $k = 1$, 2, or 3 respectively. Then,

$$\|\mathbf{G}(u,v,\Delta)\|^2 = \sum_{k=1}^{3} \left[\psi_k(\Delta) - \sum_{i=1}^{4} \sum_{j=1}^{4} B_i(u) \Lambda_{ij}^k B_j(v) \right]^2$$

where ψ_k was defined in appendix B,

$$\begin{aligned}
\frac{\partial \|\mathbf{G}\|^2}{\partial u'} &= -2 \sum_{k=1}^{3} \left\{ \left[\psi_k - \sum_{i,j=1}^{4} B_i(u) \Lambda_{ij}^k B_j(v) \right] \sum_{i,j=1}^{4} \left[\frac{\partial B_i(u)}{\partial u'} \Lambda_{ij}^k B_j(v) \right. \right. \\
&\quad \left. \left. + B_i(u) \Lambda_{ij}^k \frac{\partial B_j(v)}{\partial u'} \right] \right\}, \\
\frac{\partial^2 \|\mathbf{G}\|^2}{\partial u' \partial \Delta} &= -2 \sum_{k=1}^{3} \left\{ (X_2^k - X_1^k) \sum_{i,j=1}^{4} \left[\frac{\partial B_i(u)}{\partial u'} \Lambda_{ij}^k B_j(v) + B_i(u) \Lambda_{ij}^k \frac{\partial B_j(v)}{\partial u'} \right] \right\}, \\
\frac{\partial^2 \|\mathbf{G}\|^2}{\partial u'^2} &= -2 \sum_{k=1}^{3} \left\{ \left[\psi_k - \sum_{i,j=1}^{4} B_i(u) \Lambda_{ij}^k B_j(v) \right] \sum_{i,j=1}^{4} \left[\frac{\partial^2 B_i(u)}{\partial u'^2} \Lambda_{ij}^k B_j(v) \right. \right. \\
&\quad \left. + 2 \frac{\partial B_i(u)}{\partial u'} \Lambda_{ij}^k \frac{\partial B_j(v)}{\partial u'} + B_i(u) \Lambda_{ij}^k \frac{\partial^2 B_j(v)}{\partial u'^2} \right] \\
&\quad \left. - \sum_{i,j=1}^{4} \left[\frac{\partial B_i(u)}{\partial u'} \Lambda_{ij}^k B_j(v) + B_i(u) \Lambda_{ij}^k \frac{\partial B_j(v)}{\partial u'} \right]^2 \right\}, \\
\frac{\partial^3 \|\mathbf{G}\|^2}{\partial u'^3} &= -2 \sum_{k=1}^{3} \left\{ \left[\psi_k - \sum_{i,j=1}^{4} B_i(u) \Lambda_{ij}^k B_j(v) \right] \sum_{i,j=1}^{4} \left[\frac{\partial^3 B_i(u)}{\partial u'^3} \Lambda_{ij}^k B_j(v) \right. \right.
\end{aligned}$$

Appendix C

$$+3\frac{\partial^2 B_i(u)}{\partial u'^2}\Lambda^k_{ij}\frac{\partial B_j(v)}{\partial u'}+3\frac{\partial B_i(u)}{\partial u'}\Lambda^k_{ij}\frac{\partial^2 B_j(v)}{\partial u'^2}+B_i(u)\Lambda^k_{ij}\frac{\partial^3 B_j(v)}{\partial u'^3}\Bigg]$$
$$-3\sum_{i,j=1}^{3}\left[\frac{\partial B_i(u)}{\partial u'}\Lambda^k_{ij}B_j(v)+B_i(u)\Lambda^k_{ij}\frac{\partial B_j(v)}{\partial u'}\right]\sum_{i,j=1}^{4}$$
$$\left[\frac{\partial^2 B_i(u)}{\partial u'^2}\Lambda^k_{ij}B_j(v)+2\frac{\partial B_i(u)}{\partial u'}\Lambda^k_{ij}\frac{\partial B_j(v)}{\partial u'}+B_i(u)\Lambda^k_{ij}\frac{\partial^2 B_j(v)}{\partial u'^2}\right]\Bigg\}.$$

The expressions for $\frac{\partial^2\|\mathbf{G}\|^2}{\partial v'^2}$ and $\frac{\partial^2\|\mathbf{G}\|^2}{\partial v'\partial\Delta}$ can be obtained directly from the expressions for $\frac{\partial^2\|\mathbf{G}\|^2}{\partial u'^2}$ and $\frac{\partial^2\|\mathbf{G}\|^2}{\partial u'\partial\Delta}$ respectively by replacing u' with v' throughout:

$$\frac{\partial^3\|\mathbf{G}\|^2}{\partial u'^2\partial v'} = -2\sum_{k=1}^{3}\Bigg\{\left[\psi_k-\sum_{i,j=1}^{4}B_i(u)\Lambda^k_{ij}B_j(v)\right]\sum_{i,j=1}^{4}\Bigg[\frac{\partial^2 B_i(u)}{\partial u'^2}\Lambda^k_{ij}\frac{\partial B_j(v)}{\partial v'}$$
$$+\frac{\partial^3 B_i(u)}{\partial u'^2\partial v'}\Lambda^k_{ij}B_j(v)+2\frac{\partial B_i(u)}{\partial u'}\Lambda^k_{ij}\frac{\partial^2 B_j(v)}{\partial u'\partial v'}+2\frac{\partial^2 B_i(u)}{\partial u'\partial v'}\Lambda^k_{ij}\frac{\partial B_j(v)}{\partial u'}$$
$$+B_i(u)\Lambda^k_{ij}\frac{\partial^3 B_j(v)}{\partial u'^2\partial v'}+\frac{\partial B_i(u)}{\partial v'}\Lambda^k_{ij}\frac{\partial^2 B_j(v)}{\partial u'^2}+\Bigg]-\sum_{i,j=1}^{4}\Bigg[\frac{\partial B_i(u)}{\partial v'}\Lambda^k_{ij}B_j(v)$$
$$+B_i(u)\Lambda^k_{ij}\frac{\partial B_j(v)}{\partial v'}\Bigg]\sum_{i,j=1}^{4}\Bigg[\frac{\partial^2 B_i(u)}{\partial u'^2}\Lambda^k_{ij}B_j(v)+2\frac{\partial B_i(u)}{\partial u'}\Lambda^k_{ij}\frac{\partial B_j(v)}{\partial u'}$$
$$+B_i(u)\Lambda^k_{ij}\frac{\partial^2 B_j(v)}{\partial u'^2}\Bigg]-2\sum_{i,j=1}^{4}\left[\frac{\partial B_i(u)}{\partial u'}\Lambda^k_{ij}B_j(v)+B_i(u)\Lambda^k_{ij}\frac{\partial B_j(v)}{\partial u'}\right]$$
$$\sum_{i,j=1}^{4}\left[\frac{\partial B_i(u)}{\partial u'}\Lambda^k_{ij}\frac{\partial B_j(v)}{\partial v'}+\frac{\partial^2 B_i(u)}{\partial u'\partial v'}\Lambda^k_{ij}B_j(v)+B_i(u)\Lambda^k_{ij}\frac{\partial^2 B_j(v)}{\partial u'\partial v'}\right.$$
$$\left.+\frac{\partial B_i(u)}{\partial v'}\Lambda^k_{ij}\frac{\partial B_j(v)}{\partial u'}\right]\Bigg\}.$$

It remains to determine the various partial derivatives $\frac{\partial^{i+j}B(u)}{\partial u'^i\partial v'^j}$ and $\frac{\partial^{i+j}B()}{\partial u'^i\partial v'^j}$. First note that $\frac{\partial u}{\partial u'}=\cos\theta$, $\frac{\partial u}{\partial v'}=-\sin\theta$, $\frac{\partial v}{\partial u'}=\sin\theta$, and $\frac{\partial v}{\partial v'}=\cos\theta$ and further, that all higher order derivatives of u and v with respect to u' or v' are identically zero. It is easy to see by induction that

$$\frac{\partial^k B_i(u)}{\partial u'^k}=\frac{\partial^k B_i(u)}{\partial u^k}\left[\frac{\partial u}{\partial u'}\right]^k.$$

The basis step is

$$\frac{\partial B_i(u)}{\partial u'}=\frac{\partial B_i(u)}{\partial u}\frac{\partial u}{\partial u'}+\frac{\partial B_i(u)}{\partial v}\frac{\partial v}{\partial u'}=\frac{\partial B_i(u)}{\partial u}\frac{\partial u}{\partial u'}.$$

Appendix C

If the conjecture holds for the kth partial derivative, then

$$\begin{aligned}\frac{\partial}{\partial u'}\frac{\partial^k B^i(u)}{\partial u'^k} &= \frac{\partial^k B_i(u)}{\partial u^k} k \left[\frac{\partial u}{\partial u'}\right]^{k-1} \left[\frac{\partial^2 u}{\partial u'^2}\right] + \frac{\partial^{k+1} B_i(u)}{\partial u^{k+1}} \left[\frac{\partial u}{\partial u'}\right] \left[\frac{\partial u}{\partial u'}\right]^k \\ &= \frac{\partial^{k+1} B_i(u)}{\partial u^{k+1}} \left[\frac{\partial u}{\partial u'}\right]^{k+1}.\end{aligned}$$

Similarly,

$$\frac{\partial^k B_i(v)}{\partial v'^k} = \frac{\partial^k B_i(v)}{\partial v^k} \left[\frac{\partial v}{\partial v'}\right]^k,$$

$$\frac{\partial^k B_i(u)}{\partial v'^k} = \frac{\partial^k B_i(u)}{\partial u^k} \left[\frac{\partial u}{\partial v'}\right]^k,$$

$$\frac{\partial^k B_i(v)}{\partial u'^k} = \frac{\partial^k B_i(v)}{\partial v^k} \left[\frac{\partial v}{\partial u'}\right]^k.$$

And further, it can be shown that

$$\begin{aligned}\frac{\partial^{k+l} B_i(u)}{\partial u'^k \partial v'^l} &= \frac{\partial^{k+l} B_i(u)}{\partial u^{k+l}} \left[\frac{\partial u}{\partial u'}\right]^k \left[\frac{\partial u}{\partial v'}\right]^l \\ &= \frac{\partial^{k+l} B_i(u)}{\partial u^{k+l}} (\cos\theta)^k (-\sin\theta)^l\end{aligned}$$

and

$$\begin{aligned}\frac{\partial^{k+l} B_i(v)}{\partial u'^k \partial v'^l} &= \frac{\partial^{k+l} B_i(v)}{\partial v^{k+l}} \left[\frac{\partial v}{\partial u'}\right]^k \left[\frac{\partial v}{\partial v'}\right]^l \\ &= \frac{\partial^{k+l} B_i(v)}{\partial v^{k+l}} (\sin\theta)^k (\cos\theta)^l.\end{aligned}$$

DISTRIBUTION

ADMINISTRATOR
DEFENSE TECHNICAL INFORMATION CENTER
ATTN DTIC-DDA (12 COPIES)
CAMERON STATION, BUILDING 5
ALEXANDRIA, VA 22304-6145

COMMANDER
US ARMY ARMAMENT, MUNITIONS, &
CHEMICAL COMMAND
ATTN DRSMC-LEP-L, TECHNICAL LIBRARY
ATTN DRSMC-ASF, FUZE & MUNITIONS
SUPPORT DIV
ROCK ISLAND, IL 61299

DEPT OF THE AIR FORCE, HQ
6585TH TEST GROUP (AFSC)
RADAR TARGET SCATTER FACILITY
ATTN LT COL RONALD L. KERCHER, CHIEF
HOLLOMAN AFB, NM 88330

ENGINEERING SOCIETIES LIBRARY
ATTN ACQUISITIONS DEPARTMENT
345 EAST 47TH STREET
NEW YORK, NY 10017

DIRECTOR
DEFENSE ADVANCED RESEARCH
PROJECTS AGENCY
ARCHITECT BLDG
ATTN TARGET ACQUISITION
& ENGAGEMENT DIV
1400 WILSON BLVD
ARLINGTON, VA 22209

OFF OF THE ASSISTANT SECRETARY
OF THE ARMY (RDA)
ATTN DEP FOR COMMUNICATIONS
& TARGET ACQUISITION
WASHINGTON, DC 20310-0103

COMMANDING OFFICER
US ARMY FOREIGN SCIENCE
& TECHNOLOGY CENTER
FEDERAL OFFICE BLDG
ATTN AMXST-SC, SCIENCES DIV
220 7TH STREET, NE
CHARLOTTESVILLE, VA 22901

COMMANDER
US ARMY MISSILE COMMAND
ATTN DRCPM-CF, CHAPARRAL/FAAR

COMMANDER
US ARMY MISSILE COMMAND (Cont'd)
ATTN DRCPM-ROL, ROLAND
ATTN DRSMI-T, TARGETS MANAGEMENT OFFICE
REDSTONE ARSENAL, AL 35809

DIRECTOR
US ARMY MISSILE LABORATORY
USAMICOM
ATTN DRSMI-RD, SYS SIMULATION & DEV DIR
REDSTONE ARSENAL, AL 35809

ASSISTANT SECRETARY OF THE NAVY
RESEARCH, ENGINEERING, & SYSTEMS
DEPT OF THE NAVY
WASHINGTON, DC 20350

US ARMY LABORATORY COMMAND
ATTN TECHNICAL DIRECTOR, AMSLC-TD

INSTALLATION SUPPORT ACTIVITY
ATTN LEGAL OFFICE, SLCIS-CC

USAISC
ATTN RECORD COPY, ASNC-LAB-TS
ATTN TECHNICAL REPORTS BRANCH, ASNC-LAB-TR
(2 COPIES)

HARRY DIAMOND LABORATORIES
ATTN D/DIVISION DIRECTORS
ATTN LIBRARY, SLCHD-TL (3 COPIES)
ATTN LIBRARY, SLCHD-TL (WOODBRIDGE)
ATTN CHIEF, SLCHD-NW-E
ATTN CHIEF, SLCHD-NW-EH
ATTN CHIEF, SLCHD-NW-EP
ATTN CHIEF, SLCHD-NW-ES
ATTN CHIEF, SLCHD-NW-R
ATTN CHIEF, SLCHD-NW-CS
ATTN CHIEF, SLCHD-NW-RP
ATTN CHIEF, SLCHD-NW-RS
ATTN CHIEF, SLCHD-NW-TN
ATTN CHIEF, SLCHD-NW-TS
ATTN CHIEF, SLCHD-NW-P
ATTN D. R. COOK, SLCHD-ST-AA
ATTN J. BRUNO, SLCHD-ST-AP
ATTN H. C. LISINSKI, SLCHD-ST-SA (10 COPIES)
ATTN J. W. MILLER, SLCHD-TA-SS
ATTN R. D. CHRISTOPHERSON, SLCHD-TA-SS
ATTN K. REINIG, SLCHD-ST-SA (30 COPIES)